

**AD-A168 497**

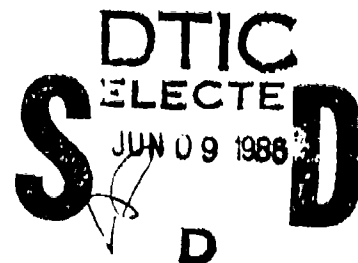
12  
DNA-TR-84-439

## **CONSIDERATIONS IN SCALE-MODELING OF LARGE URBAN FIRES**

**A. M. Kanury  
University of Notre Dame  
Department of Aerospace & Mechanical Engineering  
Notre Dame, IN 46556**

**15 November 1984**

**Technical Report**



**CONTRACT No. DNA 001-82-C-0133**

Approved for public release;  
distribution is unlimited.

THIS WORK WAS SPONSORED BY THE DEFENSE NUCLEAR AGENCY  
UNDER RDT&E RMSS CODE B345082466 G54CAXYX00007 H2590D

**Prepared for  
Director  
DEFENSE NUCLEAR AGENCY  
Washington, DC 20305-1000**

Destroy this report when it is no longer needed. Do not return to sender.

PLEASE NOTIFY THE DEFENSE NUCLEAR AGENCY,  
ATTN: STTI, WASHINGTON, DC 20305-1000, IF YOUR  
ADDRESS IS INCORRECT, IF YOU WISH IT DELETED  
FROM THE DISTRIBUTION LIST, OR IF THE ADDRESSEE  
IS NO LONGER EMPLOYED BY YOUR ORGANIZATION.



## DISTRIBUTION LIST UPDATE

This mailer is provided to enable DNA to maintain current distribution lists for reports. We would appreciate your providing the requested information.

- ☐ Add the individual listed to your distribution list.
- ☐ Delete the cited organization/individual.
- ☐ Change of address.

NAME: \_\_\_\_\_

ORGANIZATION: \_\_\_\_\_

### OLD ADDRESS

### CURRENT ADDRESS

\_\_\_\_\_  
\_\_\_\_\_  
\_\_\_\_\_

\_\_\_\_\_  
\_\_\_\_\_  
\_\_\_\_\_

TELEPHONE NUMBER: (     ) \_\_\_\_\_

SUBJECT AREA(s) OF INTEREST:

\_\_\_\_\_  
\_\_\_\_\_  
\_\_\_\_\_

\_\_\_\_\_  
\_\_\_\_\_  
\_\_\_\_\_

DNA OR OTHER GOVERNMENT CONTRACT NUMBER: \_\_\_\_\_

CERTIFICATION OF NEED-TO-KNOW BY GOVERNMENT SPONSOR (if other than DNA):

SPONSORING ORGANIZATION: \_\_\_\_\_

CONTRACTING OFFICER OR REPRESENTATIVE: \_\_\_\_\_

SIGNATURE: \_\_\_\_\_

UNCLASSIFIED

SECURITY CLASSIFICATION OF THIS PAGE

## REPORT DOCUMENTATION PAGE

Form Approved  
OMB No. 0704-0188  
Exp. Date: Jun 30, 1986

1a REPORT SECURITY CLASSIFICATION UNCLASSIFIED		1b RESTRICTIVE MARKINGS	
2a SECURITY CLASSIFICATION AUTHORITY N/A since Unclassified		3 DISTRIBUTION/AVAILABILITY OF REPORT Approved for public release; distribution is unlimited.	
2b DECLASSIFICATION/DOWNGRADING SCHEDULE N/A since Unclassified			
4 PERFORMING ORGANIZATION REPORT NUMBER(S)		5 MONITORING ORGANIZATION REPORT NUMBER(S) DNA-TR-84-439	
6a NAME OF PERFORMING ORGANIZATION University of Notre Dame	6b OFFICE SYMBOL (if applicable)	7a NAME OF MONITORING ORGANIZATION Director Defense Nuclear Agency	
6c ADDRESS (City, State, and ZIP Code) Department of Aerospace and Mechanical Engineering Notre Dame, IN 46556		7b ADDRESS (City, State, and ZIP Code) Washington, DC 20305-1000	
8a NAME OF FUNDING SPONSORING ORGANIZATION	8b OFFICE SYMBOL (if applicable)	9 PROCUREMENT INSTRUMENT IDENTIFICATION NUMBER DNA 001-82-C-0133	
8c ADDRESS (City, State, and ZIP Code)		10 SOURCE OF FUNDING NUMBERS	
		PROGRAM ELEMENT NO 62715H	PROJECT NO G54CAXY
		TASK NO X	WORK UNIT ACCESSION NO DH006015
11 TITLE (Include Security Classification) CONSIDERATIONS IN SCALE-MODELING OF LARGE URBAN FIRES			
12 PERSONAL AUTHOR(S) Kanury, A. M.			
13a TYPE OF REPORT Technical	13b TIME COVERED FROM 820501 TO 841031	14 DATE OF REPORT (Year, Month, Day) 841115	15 PAGE COUNT 102
16 SUPPLEMENTARY NOTATION This work was sponsored by the Defense Nuclear Agency under RDT&E RMSS Code 8345082466 G54CAXYX00007 H2590D.			
17 COSATI CODES		18 SUBJECT TERMS (Continue on reverse if necessary and identify by block number)	
FIELD	GROUP	SUB-GROUP	
13	12		
		Fire Urban Fires Scaling Modeling	
19 ABSTRACT (Continue on reverse if necessary and identify by block number) The feasibility of scale-modeling a large urban fire is examined by critically reviewing some of the most important existing fire study reports and papers on various aspects ranging from ignition to a fully-developed mass fire. The review process led to extracting valuable scaling information on each aspect. Not unexpectedly, however, it is found that complete modeling of the entire chronological development of the fire is impossible due to conflicting scale restraints and due to limited degrees of freedom of the experimenter. Partial modeling of selected aspects is not only possible but also promising. Among the most crucial aspects in which the existing knowledge is inadequate to develop scaling rules is the behavior of firebrand production in a fire and combustive consumption in its flight.			
20 DISTRIBUTION AVAILABILITY OF ABSTRACT <input type="checkbox"/> UNCLASSIFIED UNLIMITED <input type="checkbox"/> SAME AS RPT <input type="checkbox"/> D. C. USERS		21 ABSTRACT SECURITY CLASSIFICATION UNCLASSIFIED	
22a NAME OF RESPONSIBLE INDIVIDUAL Betty L. Fox		22b TELEPHONE (Include Area Code) (202) 325-7042	22c OFFICE SYMBOL DNA/STTI

DD FORM 1473, 34 MAR

If APP edition may be used until exhausted  
All other editions are obsolete

SECURITY CLASSIFICATION OF THIS PAGE

UNCLASSIFIED

# CONVERSION TABLE

Conversion factors for U.S. Customary to metric (SI) units of measurement

MULTIPLY → BY → TO GET  
TO GET ← BY ← DIVIDE

angstrom	1.000 000 X E -10	meters (m)
atmosphere (normal)	1.013 25 X E +2	kilo pascal (kPa)
bar	1.000 000 X E +2	kilo pascal (kPa)
bern	1.000 000 X E -28	meter <sup>2</sup> (m <sup>2</sup> )
British thermal unit (thermochemical)	1.054 350 X E +3	joule (J)
calorie (thermochemical)	4.184 000	joule (J)
cal (thermochemical)/cm <sup>2</sup>	4.184 000 X E -2	mega joule/m <sup>2</sup> (MJ/m <sup>2</sup> )
curie	3.700 000 X E +1	*giga becquerel (GBq)
degree (angle)	1.745 329 X E -2	radian (rad)
degree Fahrenheit	$t_F = (t_C + 459.67)/1.8$	degree kelvin (K)
electron volt	1.602 19 X E -19	joule (J)
erg	1.000 000 X E -7	joule (J)
erg/second	1.000 000 X E -7	watt (W)
foot	3.048 000 X E -1	meter (m)
foot-pound-force	1.355 818	joule (J)
gallon (U.S. liquid)	3.785 412 X E -3	meter <sup>3</sup> (m <sup>3</sup> )
inch	2.540 000 X E -2	meter (m)
jerk	1.000 000 X E +9	joule (J)
joule/kilogram (J/kg) (radiation dose absorbed)	1.000 000	Gray (Gy)
kilotons	4.183	terajoules
ktp (1000 tbf)	4.448 222 X E +3	newton (N)
ktp/inch <sup>2</sup> (ksi)	6.894 757 X E +3	kilo pascal (kPa)
ktap	1.000 000 X E +2	newton-second/m <sup>2</sup> (N-s/m <sup>2</sup> )
micron	1.000 000 X E -6	meter (m)
mil	2.540 000 X E -5	meter (m)
mile (international)	1.609 344 X E +3	meter (m)
ounce	2.834 952 X E -2	kilogram (kg)
pound-force (lbs avoirdupois)	4.448 222	newton (N)
pound-force inch	1.129 848 X E -1	newton-meter (N-m)
pound-force/inch	1.751 268 X E +2	newton/meter (N/m)
pound-force/foot <sup>2</sup>	4.788 026 X E -2	kilo pascal (kPa)
pound-force/inch <sup>2</sup> (psi)	6.894 757	kilo pascal (kPa)
pound-mass (lbm avoirdupois)	4.535 924 X E -1	kilogram (kg)
pound-mass-foot <sup>2</sup> (moment of inertia)	4.214 011 X E -2	kilogram-meter <sup>2</sup> (kg-m <sup>2</sup> )
pound-mass/foot <sup>3</sup>	1.601 846 X E +1	kilogram/meter <sup>3</sup> (kg/m <sup>3</sup> )
rad (radiation dose absorbed)	1.000 000 X E -2	**Gray (Gy)
roentgen	2.579 760 X E -4	coulomb/kilogram (C/kg)
shake	1.000 000 X E -8	second (s)
slug	1.459 390 X E +1	kilogram (kg)
torr (mm Hg, 0° C)	1.333 22 X E -1	kilo pascal (kPa)

\*The becquerel (Bq) is the SI unit of radioactivity; 1 Bq = 1 event/s.  
\*\*The Gray (Gy) is the SI unit of absorbed radiation.



For	
RA&I	<input checked="" type="checkbox"/>
B	<input type="checkbox"/>
ed	<input type="checkbox"/>
Availability Codes	
Dist	Avail and/or Special
A-1	

# TABLE OF CONTENTS

Section	Page
CONVERSION TABLE. . . . .	iii
1. INTRODUCTION . . . . .	1
2. NATURE OF THE EXPECTED FIRE . . . . .	2
3. DIMENSIONAL REASONING . . . . .	4
4. CERTAIN LIMITATIONS IN DIMENSIONAL REASONING APPLIED TO THE PHENOMENON OF FIRE . . . . .	7
5. IRRADIANCE FROM THE FIREBALL TO THE TARGET . . . . .	9
6. IGNITION . . . . .	14
7. IMPACT OF THE BLAST WAVE ON THE NASCENT FIRES . . . . .	19
8. FIRE PROPAGATION AND GROWTH . . . . .	25
8.1 Spread of a Fire by a Smolder Front . . . . .	25
8.2 Horizontal and Downward Flame Spread in Opposing Wind . . . . .	27
8.3 Upward Fire Spread on Vertical Surfaces . . . . .	30
8.4 Fire Spread in a Forest . . . . .	32
8.5 Fire Growth in Compartments . . . . .	41
8.6 Radiant Heating and Jumping Fire Spread . . . . .	45
9. MASS FIRE . . . . .	47
9.1 Dynamics of Plumes over 'Small' Turbulent Fires . . . . .	47
9.2 Radiative Effects in Plumes . . . . .	51
9.3 Induced Wind Flow: Some Estimates and Some Measurements . . . . .	54
9.4 Firebrand Transport . . . . .	58
9.5 Fire and Wind/Firestorms . . . . .	60
9.6 The Combustion Zone Specifics . . . . .	63
10. CONCLUDING REMARKS . . . . .	70
11. LIST OF REFERENCES . . . . .	72
Appendix GLOSSARY OF TERMS . . . . .	79

## SECTION 1

### INTRODUCTION

The objective of the present work is to assess the feasibility of studying the blast, fire, and wind effects due to a nuclear explosion in an urban setting by employing scale-modeling techniques. Our concentration will be on fire-scaling. The blast effects will be considered only to the extent of concern to describe the initial combustibles distribution near ground-zero. In a similar way, the winds produced directly by the explosion will be considered only as to their impact on the initial fires. As the blast wave passes and the associated winds subside, the fire would develop in a self-regulated manner involving complicated heat transfer, turbulent buoyant fluid mechanics and combustion. It is this development upon which we focus attention.

Existing literature indicates that knowledge about the behavior of fire following a nuclear explosion is less complete than about the blast and radioactive fall out. A nuclear explosion triggers fires in an urban area by two different mechanisms: First, primary fires are initiated due to thermal radiation emitted by the fire-ball over an area in close enough proximity to ground-zero where the irradiance is sufficiently high to heat the combustibles to the state of ignition. These nascent fires are then subjected, within seconds, to the blast effects of wind, pressure-rise and mechanical disruption. The consequence may be either extinguishment or augmentation of the fires. Second, secondary fires are initiated as the blast damages the mechanical systems in and outside the structures physically. Broken gas pipes, fallen electrical wires, ruptured chemical storage/transportation equipment and others constitute the sources of secondary fires.

Fires associated with nuclear blasts are characteristically expected to continue burning long after the blast effects subside. Once the primary ignitions are modified by the blast wave and the secondary ignitions are provoked, the individual fires are expected to grow to coalesce together. In this coalescing process, such phenomena as flashover in enclosures (i.e., rooms), penetration through walls, fire-jumping across breaks in the fuel bed are generally involved in addition to fire propagation over contiguous fuel beds. Once coalesced, the resultant area-fire will conflagrate to result in a mass fire.

## SECTION 2

### NATURE OF THE EXPECTED FIRE

Thermally thin combustibles are generally expected to be the first ignited items no matter whether they are situated indoors or outdoors. These include window coverings, upholstery linings, carpets, papers, fabrics, grasses, leaves, dry shrubs, etc. The criterion by which thermal thickness is judged is based on whether or not internal temperature gradients predominate within the solid. The nondimensional parameters addressing this issue is known as Biot number which is discussed in detail in a later chapter of this report. Suffice it to say, thermally thin bodies are characterized by a Biot number much smaller than unity.

As energy impinges on the solid surface, part of it is reflected, part is lost by convection and the rest is employed to heat the body by conduction to ignition. The heated body may also suffer reradiative loss. If the intensity of irradiance is high, heating to ignition occurs so fast as not to provide time to develop the natural convective heat loss process. The ignition process has been studied extensively by experiment (Martin [1]) and by analysis (Kanury [2], Gandhi [3]).

Once the fire is thus initiated, it will grow. If the initial ignition is indoors, the fire growth process is influenced by the room configuration. This influence is weak initially and strong in later stages leading towards what is known as flashover. Room fire flashover is extensively studied experimentally, analytically and by scaling (Kanury [4]). an interesting additional feature of flashover in rooms exposed to the fire-ball is the role played by the radiant deposition of energy on the unignited combustibles of the room. This role is surmised by Martin to expedite the arrival of flashover. The scaling considerations of flashover will be discussed later in detail.

If the fire were in the open, such as in a grassy field or in a forest, the initial fire growth follows the pattern of a conflagration at a small scale. The scaling rules governing this growth are also discussed later from the basis of the existing knowledge on fire spread and forest fires.

As the fire from the initial ignitions thus attempts to evolve, the blast would soon arrive to disrupt it. The effect of blast impingement is known to be towards extinguishing the gas-phase flames and augmenting glowing-type solid-phase (or near surface) phenomena (Kanury [5]). Even more importantly, the blast wave would disrupt the burning fuel elements perhaps to a geometrical configuration more conducive to intensified burning and would



produce secondary ignitions to augment the fire.

Finally, as the fire flashes over in rooms and penetrates through walls, fire spread from structure to structure becomes relevant in the development of the conflagration and mass fire. Thermal radiative heat transfer becomes crucial in this spread process. Scaling considerations of both the radiative (conflagratory) fire spread and the mass fire will be subject to discussion in later sections.

## SECTION 3

### DIMENSIONAL REASONING

As one embarks upon the task of developing a quantitative understanding of the process of inception and growth of an urban fire, one encounters a number of choices as to the level and detail of study. Since the fire phenomenon is a complicated mosaic of several component processes, one can choose an isolated process for a detailed theoretical and experimental study. The more the numbers of interacting component processes considered, the less amenable the study becomes to a detailed analysis. But because one is often concerned with the behavior of a real fire, albeit complex, one is faced with the need to synthesize a number of nonlinear processes into a comprehensive whole. Modern high speed computers have become extremely useful in this synthesis. Experimental methods, however, leave much to be desired in their sophistication, for real fires are 'dirty' and perhaps will always remain benefited from the modern developments in instrumentation technology. What is possible, however, is powerful data acquisition, quick analysis and instructive presentation.

While endeavors in theoretical analysis of fires will become gradually more sophisticated, experimentation will continue to provide not only the input data required in theories but also the output to validate theories.

The terms 'modeling' (broadly) and 'scaling' (specifically) are traditionally used to describe the endeavors associated with attempts to design experiments on a systematic foundation and to present the data from a limited number of experiments in a generalizable form suggestive of the involved mechanisms. Modeling (scaling) is a valuable technique to understand the outcome of the prototype experiment which is generally prohibitive in cost, material, and time, or when it involves scales of time, mass and size that are difficult to be contrived in an experimental set-up. Simulation and analog modeling techniques are capable of yielding a convenient, controlled, inexpensive, and meaningful model experiment in which the phenomena of interest can be highlighted.

Note that the term scale model implies more than the general connotation of miniature hardware. The design of scale model experiments requires an identification of the constraint parameters which have to be preserved invariant between the model and prototype experiments. These parameters are nondimensional ratios of fluxes, forces, lengths or of time constants. Identification of these parameters generally requires an enumeration of the

involved variables but not a quantitative relation among them.

Scale model studies of any physico-chemical system offer one or more of the following four advantages: (a) attack is possible on such new, unexplored and complex problems which are not amenable to an analytic formulation and solution; (b) transformation to physically manageable geometric proportions is possible of such systems which are too extensive to permit direct experimentation; (c) time scales can be expanded or contracted to speed-up (or slow-down) the processes which are too slow (or too fast) for direct experimentation; and (d) since model experiments can be conducted redundantly under well-controlled conditions, the phenomenon under scrutiny can be understood much more deeply.

Design of scale model experiments requires a preliminary, order-of-magnitude analysis of the underlying physico-chemical mechanism(s) of a phenomenon. As such, the endeavor of designing a scale model experiment squarely falls on the boundary between theoretical analysis and experimental study.

The idea of order-of-magnitude analyses of a process automatically invokes that the various terms in an equation governing the process behavior must all be of the same magnitude under the extreme conditions of the process. This would imply that prior to being able to conduct an order-of-magnitude analysis, one has to be able to postulate a hypothesis upon the basis of which the concerned process occurs and to put this hypothesis in the form of a simple (or complex) governing equation. A correct governing equation has to satisfy two basic requirements: first, all of its terms must be of equal magnitudes. This requirement results from retaining only those terms which represent importance in the governance of the process while ignoring terms standing for unimportant or secondary aspects. Recognition of which terms to drop out and which to keep is an important skill of a knowledgeable physicist. Second, the governing equation has to be dimensionally homogeneous; that is, all of its terms have the same units.

These two requirements lead to the following two axioms which form the foundation piers of the art of 'dimensional analysis' (Murphy [6]).

1. Absolute numerical equality of quantities may exist only when the two quantities are qualitatively similar. (That is, an apple may be equal to another apple but never to an orange!)

2. The ratio of magnitudes of two like quantities is independent of the units used in their measurement, provided that the same units are used for

evaluating each. (For example, the length and width of a table are like quantities; both have units of L; the ratio of length to width is same no matter whether one measured them in inches, feet, yards, meters or miles.)

Based on these two axioms, the powerful tool of dimensional analysis evolved to enable deduction of qualitative relationships among the process variables. These relationships guide the investigator to design experiments which yield maximum generalizable data with an economy of time and resources. The experimental data in the framework of the qualitative relationships lead to quantitative results and even predictive rules.

Thus, to be able to make dimensional and/or order-of-magnitude analyses of a given process, one first needs enough of an understanding of the process to identify the component forces and fluxes. Any attempt to make an order-of-magnitude estimate is invariably a prelude to deducing the nondimensional scale parameters of the problem and their expected quantitative range. As Segel [7] enumerates, there exist at least six different ways to obtain the preliminary understanding of any given process: (a) utilize experimental and observational evidence related to the process; (b) use experience from related or analogous problems; (c) solve simplified versions of the problem; (d) ignore terms which are small in order-of-magnitude and solve the resulting simpler problem; compare the solution with experiments and justify that the ignored terms are indeed small; (e) assume certain scaling; solve the problem; check if the dimensionless terms are of magnitude unity; and if any of them are not, refine the assumed scaling; and (f) examine the complete (or comprehensive) numerical solutions to identify the scaling parameters.

## SECTION 4

### CERTAIN LIMITATIONS IN DIMENSIONAL REASONING APPLIED TO THE PHENOMENON OF FIRE

The concepts of dimensional reasoning discussed in the preceding chapter are indeed powerful in solving numerous problems in science and engineering. Much progress has been made in fire studies also. There exist, however, several limitations of the modeling technique when dealing with fire phenomena. It is worthwhile to formally identify and constantly remember these limitations.

Combustion phenomena involve a host of physico-chemical processes including heat and species diffusion, viscosity effects, buoyancy, surface tension, compressibility, kinematics and dynamics, heterogeneous and homogeneous reactions, equilibria, heat and mass transfer to (or from) the boundaries, thermal radiation, condensation and evaporation, particle agglomeration, and others. If the characteristic rates (or times) for these various processes can be identified, then one can obtain the relative measure of any of these processes with respect to any other in the form of nondimensional groups. Spalding [8] identifies 105 such groups which may have an apparent relevance in a general combustion scaling problem. It is fitting to note that the various physical and chemical processes deemed to arise in combustion have been identified intuitively by Spalding.

F. A. Williams [9], in contrast, considers the mass fire problem which is somewhat more specific in many respects and yet more complex in other respects than Spalding's general combustion problem. Based on equations of change, Williams identifies a total of 29 nondimensional groups,\* 19 of which arise from the conservation equations themselves and 10 from the boundary conditions. (Of these last 10, six pertain to the fuel element description and four to the ambient atmosphere.)

Since these many identifiable nondimensional groups far surpass the experimentally plausible degrees of freedom, one has to discern the scaling groups which need not be preserved invariant between the model and the

---

\*Williams' enumeration in fact involves far more than 29 groups, the actual number being determined by the total number of concerned chemical species.

prototype experiments. It is in this discernment that one needs physical insight and practical experience. It is also in this discernment that one recognizes the impossibility of complete modeling of a combustion problem and the need to be satisfied with 'partial modeling'.

Even partial modeling is seldom possible of the entire chronological behavior of a fire from ignition to sustainment to spread and growth to quasi-steady burning to subsidence and extinguishment. One is thus forced to concentrate on one stage of the fire -- say, steady burning -- or one aspect of it -- say, the burning intensity -- and settle to model it partially. It is not at all uncommon to discover that the scaling constraints fulfilling the requirements of similarity between the model and prototype with respect to one aspect of fire behavior may conflict with restraints to obtain similarity of another aspect. For example, scaling rules to reproduce the convective effects are generally incompatible with those to preserve the thermal radiation effects.

Thus, as Spalding concludes, the permissibility of a particular scaling technique depends for the most part on the stated limited objectives of the study and accuracy sought.

The scaling considerations discussed in the rest of this report are based on the premise of partial modeling. As such, the discussion follows the scaling restraints associated with various chronological aspects of the fire in the respective independent sections.

In each section, the most significant existing knowledge is identified and this knowledge is converted into a scaling exercise to identify the similarity groups which are important in the design of a scale model experiment.

## SECTION 5

### IRRADIANCE FROM THE FIREBALL TO THE TARGET

Thermal radiation from the air burst of a nuclear weapon comes in its characteristic double-peak (Glasstone/Dolan [10]) to heat all the materials exposed to it. It is well-known (Martin [11]) that the second temporal peak contributes most to this heating process. If the heated materials are combustible, they pyrolyze and spontaneously ignite within the range where the thermal fluence exceeds about 12 Joules/cm<sup>2</sup>. Delineation of this range requires an examination of three aspects: first, the characteristics of the fireball as a source of thermal radiation; second, transmission of the emitted thermal radiation through the atmosphere to the target combustible materials; and third, the thermal response and ignition behavior of the exposed materials. In this chapter, we deal with the first two of these three aspects deferring consideration of the third to the following chapter.

Let  $W$  be the yield of the weapon usually expressed in units of kilo-ton (kt) equivalent of TNT explosive.\* The fraction of  $W$  which is emitted as thermal radiant energy  $E_{\text{total}}$  depends not only on  $W$  itself but also on the height of burst  $H$ . Denoting this fraction by  $f$  ( $\equiv E_{\text{total}}/W$ ), Glasstone and Dolan (Page 313) present  $f = f(W, H)$  in tabular form. In general,  $f$  is larger if  $H$  and  $W$  are larger.

Of importance in incendiary effects of nuclear explosions is the manner in which thermal energy is released with respect to time. Experience indicates that the rate of thermal energy release  $P$  exhibits a maximum at a time  $t = t_{\text{max}}$  and then gradually decays. Both  $t_{\text{max}}$  and  $P_{\text{max}}$  depend upon the yield  $W$  and the height of burst  $H$ . Glasstone and Dolan give (Page 309) this dependency in the following form.

$$F = c \left( \frac{\rho}{\rho_0} \right)^n W^m \quad (5.1)$$

where  $F$  can be either  $P_{\text{max}}$  or  $t_{\text{max}}$ .  $\rho$  is the density of air at the height of burst and  $\rho_0$  is that at the sea level. The constants  $c$ ,  $n$  and  $m$  depend on

\*1 kt TNT equivalent  $\equiv 10^{12}$  calories =  $4.186 \times 10^{12}$  Joules.

whether  $P_{\max}$  or  $f_{\max}$  is under consideration and also on whether the height of burst is below or above 15,000 ft. Table I gives these constants.

The instantaneous thermal power output  $P$  (Watts) of the fireball of instantaneous temperature  $T(K)$  and radius  $R(m)$  can be expected to be given by

$$P = 4\pi\sigma T^4 R^2 \quad (5.2)$$

where  $\sigma$  is the Stefan-Boltzmann constant ( $\sigma = 5.67 \times 10^{-8} \text{ W/m}^2\text{K}^4$ ). As  $T$  and  $R$  change with time so also does  $P$ . Apparent in this  $P(T,R)$  relation is the initial increase in  $P$  due to the increase in both  $T$  and  $R$  and the later decay due to the decrease in  $T^4$  overwhelming the increase in  $R^2$ . This temporal distribution is given by a single curve (see Fig. 7.84 on page 311 of Glasstone and Dolan) in the coordinates of  $P/P_{\max}$  versus  $t/t_{\max}$  to absorb the dependence of history on  $W$  and  $H$ .

The integral of  $P$  from  $t = 0$  to  $t$  gives the thermal energy emitted to the time  $t$  of consideration.

$$\int_0^t P(t)dt = E(t) \quad (5.3)$$

$E(\infty)$  being the quantity identified earlier by the symbol  $E_{\text{total}} \equiv fW$ . The amount of thermal energy released to time  $t$  expressed as a percentage of the total release, i.e.,  $E(t)/E(\infty)$ , is also given in the figure mentioned above. A more explicit, albeit dimensional, result of  $E(t)$  for air bursts of different yields (but at altitudes of bursts below 100,000 ft) is presented in Figure 7.87 on page 314 of Glasstone and Dolan. Evident from this figure is the dependence of  $t_{\max}$  on  $W$  which translates into the fact that explosions of high yield  $W$  result in longer pulse lengths.

Thus it is clear that once the yield  $W$  and height of burst  $H$  are given, one can read off the thermal partition  $f$  from a table to obtain the total thermal energy output  $E(\infty)$  as  $fW$ . Simultaneously, the peak power  $P_{\max}$  and the time to its occurrence  $t_{\max}$  can be calculated from the known  $c$ ,  $n$  and  $m$  of Table I. One can then enter into Figure 7.84 of Glasstone and Dolan at any time  $t$  to read off  $P(t)/P_{\max}$  as well as  $E(t)/E(\infty)$ . Having already estimated  $P_{\max}$  and  $E(\infty)$ , the instantaneous power  $P(t)$  and thermal energy release  $E(t)$  to time  $t$ , are immediately obtainable.



Table 1. The Constants of Eq. (5.1).

Burst height, ft	< 15000		>15000	
F	P <sub>max</sub> (kt/sec)	t <sub>max</sub> (sec)	P <sub>max</sub> (kt/sec)	t <sub>max</sub> (sec)
c	3.18	0.0417	3.56	0.038
n	0	0	-0.45	0.36
m	0.56	0.44	0.59	0.44

If the fireball is taken as a point source emitter, the radiant flux arriving at a target located at a distance  $D$  away,\* is given by

$$I(t) = P(t) \times \tau / 4\pi D^2 \quad (5.4)$$

where  $\tau$  is the transmissivity of the intervening air mass and the denominator stands for the area of the imaginary spherical surface. This relation is exact for a point or spherically symmetric source. When the source is real, it is a reasonable approximation for large values of  $D$ . The transmissivity  $\tau$  of the atmosphere is less than unity due to the combined effects of absorption and scattering. If scattering were absent, then  $\tau = \exp(-\kappa D)$  where  $\kappa$  is the absorption coefficient; this corresponds to an atmosphere free of clouds and moisture. Figure 7.98 of Glasstone and Dolan shows the transmissivity on a clear day as a function of the height of burst and the distance from ground zero.

The units of  $I$ , of course, are  $W/m^2$ . From the known  $P(t)$  history due to a burst of yield  $W$  at a given altitude  $H$ , applying the  $\tau(H,d)$  from Figure 7.98 of Glasstone and Dolan and knowing  $D = \sqrt{H^2 + d^2}$ , the instantaneous irradiance  $I = I(t;W,H,d)$  is thus obtainable.\*\*

Once  $I$  is mapped out, we are faced with the response of target materials exposed to it. A discussion of this response constitutes the content of the following chapter. From laboratory data on the ignition response of various materials, Martin developed the range within which ignition is possible from a 10 MT air bursts at different altitudes. This result is presented in Figure 1 on page 3.17 of Ref. [11]. The limitations associated with this development and the scaling considerations necessary to validate it with experiments are discussed in the following chapter.

\*  $D = \sqrt{H^2 + d^2}$  where  $H$  is height of burst and  $d$  is distance from ground zero.

\*\* The integral  $\int_0^t I(t)dt$  is known as fluence,  $\hat{F}(t)$  whose units are  $J/m^2$ .

This quantity physically represents the total energy deposited, from time equal to 0 to  $t$ , on a unit area of the target surface. The fluence is to irradiance as  $E$  is to power. Thus

$$\hat{F}(t) \equiv \int_0^t I(t)dt = \int_0^t P(t) \tau / 4\pi D^2 dt = E(t) \tau / 4\pi D^2.$$

With  $E(t)$  and  $\tau$  obtained respectively from Figures 7.84 and 7.98 of Glasstone and Dolan, the instantaneous fluence at any distance  $d$  from a burst of a given yield  $W$  at a height  $H$  is thus readily calculable. The total fluence  $\hat{F}(\infty)$  is simply  $E(\infty) \tau / 4\pi D^2 = fW \tau / 4\pi D^2$ .

It is clear from the preceding discussion that one can make a satisfactory estimation of the irradiance due to a single burst in the air. Existing ability to estimate the irradiance due to multiple bursts is not as satisfactory. The alteration of the atmospheric attenuation is perhaps the most difficult issue associated with this multiburst problem.

## SECTION 6

### IGNITION

Spontaneous ignition of radiantly heated combustible solids has been an extensively studied subject in the fields of both propellant combustion and fire safety. Much of the fire-related ignition study has been of experimental nature. Certain special observations have to be enumerated here.

(a) Shape of the irradiance pulse: The complicated shape of thermal energy release from an air blast discussed in the preceding chapter is difficult to reproduce in a laboratory ignition test. While the pulse shape discussed in ENW and summarized in the previous chapter of this report is reasonable at low altitudes, the pulse may be quite different in shape if the altitude of burst is high. As Martin [11] states, it is clear from a large body of experimental work that the response of materials to the ENW pulses can be correlated by techniques which apply to rectangular (or square-wave or constant-flux) pulses.

(b) First ignited materials: The extensive experimental studies reported by Martin suggest that the most crucial materials of concern in ignition by the fireball are thin cellulosic and related polymeric kindling fuels. These are generally capable of igniting within a few seconds of exposure to fluences less than about 120 W/cm<sup>2</sup>.

(c) Main controlling process: The experiments also showed that conduction of heat into the ignitable solid is the primary process controlling the spontaneous ignition due to radiant exposure. Three distinct kinds of ignition -transient flaming, persistent flaming and thin-body (glowing) ignitions -are identified as dependent upon the thickness  $\lambda$  and conductivity  $K_s$  of the specimen and the irradiance  $I$  and duration  $t$  of the exposure. Martin [1] empirically delineates the conditions under which the different kinds of ignition occur.

(d) The prominence of transient conduction in spontaneous ignition leads to infer that ignition is incipient when the exposed surface attains a prescribed ignition temperature. Based on this criterion, the present author [2] attempted to theoretically deduce Martin's map. The nondimensional parameters which require to be preserved invariant between different situations to scale the ignition process are evident from this analysis. At the minimum, they are:

$$\text{Exposure parameter} \quad I\ell/K_s(T^*-T_0) \quad (6.1)$$

$$\text{Fluence parameter} \quad I\alpha_s t/K_s(T^*-T_0)\ell \quad (6.2)$$

$$\text{Convective heat loss parameter} \quad h\ell/K_s \quad (6.3)$$

$$\text{Thermochemical parameter} \quad (T_p - T_0)/(T^* - T_0) \quad (6.4)$$

$T^*$  is the prescribed ignition temperature,  $T_0$  is the solid's initial temperature and  $T_p$  is the solid temperature at which its pyrolysis is copious.  $h$  is the convective heat loss coefficient.  $t$  is time.  $\alpha$  is thermal diffusivity. The subscript  $s$  stands for the solid.

Note that the ratio of the fluence and exposure parameters yields the well-known Fourier modulus,  $\alpha_s t/\ell^2$ , i.e., the nondimensional time as traditionally defined in diffusion problems. The exposure parameter is a characteristic Biot number which indicates the magnitude of the energy deposition rate  $I$  relative to the characteristic energy conduction rate into the solid  $K_s(T^*-T_0)/\ell$ . A physically thin solid of high conductivity and characteristic temperature difference  $(T^*-T_0)$ , when exposed to a low intensity of irradiation, results in a small exposure parameter. The solid then entertains negligible internal temperature gradients and is called 'thermally thin'. A physically thick solid of low thermal conductivity when heated intensely, results in a large value of exposure parameter. Internal temperature gradients predominate in such a 'thermally thick' solid.

Upon incorporating the definition of thermal diffusivity  $\alpha_s \equiv K_s/\rho_s C_{ps}$ , (where the denominator is the volumetric heat capacity of the solid), one can see the fluence parameter take the form  $It/\rho_s C_{ps}(T^*-T_0)\ell$ . In this form, it is evident that the fluence parameter is the ratio of total energy supplied to the solid to the energy involved in raising the solid temperature from  $T_0$  to  $T^*$ .

The convective loss parameter apparently becomes important only when the solid is thermally thin. It obviously depends upon not only the orientation of the sample with respect to gravity but also on the characteristic dimension. The gas phase thermophysical properties also intrude into the heat transfer loss coefficient  $h$ . It is interesting to note that the ratio of the loss parameter to the exposure parameter yields  $h(T^*-T_0)/I$  which represents the rate of energy loss by convection

(characteristically when  $T=T^*$ ) expressed as a fraction of the irradiant energy supply rate.

If only a restricted class of materials is of concern, then the thermochemical parameter can be taken as fixed. There are, however, approximations pertaining to the pyrolysis kinetics (via  $T_p$ ) and to the kinetics of oxidation of the pyrolyzate efflux (via  $T^*$ ) embedded in this parameter.

(e) The experience of difficulty in igniting fuels which are thick is evidently explained by the excessive conductive drain into the solid. That moist fuels are harder to ignite is also perhaps explainable through the influence of moisture on  $T^*$  and/or  $T_p$ .

(f) Even more important is the implication of points (c) and (d) that the fluence required to produce ignition is higher if the exposure flux is lower. In fact, there exists enough convincing experimental evidence to indicate that the ignition temperature  $T^*$  is not altogether a constant for a given material as embodied the delineations of Refs. [1 and 2]; and that it is higher at a lower irradiance, such a dependency being more pronounced at smaller irradiances.

(g) A serious consequence of this  $T^*(I)$  dependency is the existence of a threshold irradiance level below which ignition of the solid will not occur even with an indefinitely long duration of exposure.

(h) The issues of ignition thus are two-fold. First, does a given exposure irradiance produce ignition of a given target? Second, if the answer to the first question is in the affirmative, how long an exposure duration is required to produce ignition? While the first question is concerned with the ignition threshold, the second is with the ignition time.

A recent work by Gandhi [3] addresses these two issues. One of the accomplishments of this work is the description of the energy balance associated with heating the solid radiatively to ignition. As the solid gets heated by transient conduction, its hot surface loses energy not only by thermal reradiation to the surroundings but also by natural convection of the adjacent gas. Among the primary descriptors of the problem are: (a) the orientation of the element which influences the inception and effectiveness of the free convective loss as well as the angle of impingement of the radiant beam; (b) the exposure intensity  $I$  nondimensionalized (with the element

conductivity  $K_S$  and ambient temperature  $T_\infty$ ) to the form  $I\ell/K_S T_\infty$ ; (c) the length of the element  $H$  nondimensionalized (with the gravity constant  $g$  and gas-phase kinematic viscosity  $\nu_g$ ) to form a Galileo number  $gH^3/\nu_g^2$ ; (d) the surface emissivity  $\epsilon_S$  normalized (with the Stefan-Boltzmann constant  $\sigma$ , ambient temperature  $T_\infty$ , element thickness  $\ell$  and solid conductivity  $K_S$ ) to form  $\sigma\epsilon_S^3 T_\infty^3 \ell/K_S$ . Time  $t$  is normalized to be a Fourier modulus  $\alpha_s t/\ell^2$  where  $\alpha_s$  is the virgin solid thermal diffusivity. There are six additional parameters of secondary importance contributed by the kinetics and energetics of pyrolysis and oxidation reactions. The ratios of various thermophysical properties of the solid and gas phases constitute tertiary parameters. While a number of important predictions are possible from Gandhi's theory, it is sufficient to note here that the most crucial scaling parameters to study ignition are the following.

Orientation

---

Exposure parameter	$I\ell/K_S T_\infty$	(6.5)
--------------------	----------------------	-------

Height parameter	$gH^3/\nu_g^2$	(6.6)
------------------	----------------	-------

Reradiant loss parameter	$\sigma\epsilon_S^3 T_\infty^3 \ell/K_S$	(6.7)
--------------------------	--	-------

Thickness parameter	$\ell/H$	(6.8)
---------------------	----------	-------

Time	$\alpha_s t/\ell^2$	(6.9)
------	---------------------	-------

(i) The orientation of the target element is known to influence the possibility of ignition. Martin, for example, reports on experiments in which a given irradiance may be capable of producing ignition of a larger element in vertical orientation but may merely char without ignition when the element is horizontal or short.

(j) There exist a number of field tests in which the vulnerability of combustibles exposed to fireball radiation is monitored by employing beds of shredded paper, shaved wood and excelsior as targets. In view of the preceding discussion, the factors of concern in this practice include: (i) the bed orientation; (ii) the packing density of the bed; (iii) the bed thickness, if packing is dense; (iv) the fineness of shredding; and (v) the paper thickness.

It is obvious that two conductivities of the condensed phase become relevant; first, the effective conductivity of the porous bed and second, the conductivity of the shred element material. If packing is rather dense, it is the overall bed characteristics which govern the ignition process. If the packing is loose, on the other hand, it is the characteristics of the shred element which are critical. Design of these target beds to maximize the obtainable information is by itself an important and interesting research project.



## SECTION 7

### IMPACT OF THE BLAST WAVE ON THE NASCENT FIRES

Following the radiant ignition, the scaling of which has been discussed in the preceding chapter, the fires would grow. (Fire propagation will be discussed in the following Section. The blast wave, along with its associated transient pressure disturbance and winds, would soon arrive to impinge upon the flames which are but only in their earliest stages of growth. Whether or not the blast impingement would extinguish the flames is a question of concern.

The properties of concern in the blast/fire interaction process may be conveniently placed into three categories respectively pertaining to the fuel, fire, and the blast. Among the fuel properties are: the pyrolysis kinetics of wood fuel or the vaporization thermodynamics of liquid fuels, thermodynamics of mixing, thermochemistry of glowing and flaming combustion, oxidation kinetics of glowing and flaming reactions, and transport properties. The fire properties mainly concern the geometry (shape, size, orientation) of the fuel bed, the nature of flow (forced or free convection) and the externally imposed radiant flux. The blast properties include the peak overpressure, time of positive phase and continued radiant pulse. Naturally, the consequence of fuel beds redistributed into debris piles in a multiple blast situation is to be considered after some degree of understanding is obtained about the well-defined single fire response to a well-defined single blast impingement.

The most abundant and relevant experiments to study the blast/fire interaction process are those reported by Martin, Backovsky and their colleagues at SRI International [12-14]. The SRI experimental facility attempts to capture the essential variables; the air-driven shocktube is capable of producing shockwaves typical of those produced by kilo-to-megaton nuclear explosions in air. The peak over pressures (up to 25 psi) and positive phase durations (between 0.10 to over 3.5 sec) are prescribable by the operator in this experimental set up. Liquid pool fires are tested with a variety of fuels: n-hexane, methanol, kerosene, n-pentane, and acetone with the fuel bed length ranging between 12 and 36 inches. The mean overpressure is varied between 0.91 and 7.5 psi. Time of positive phase duration was ranged between 0.068 and 3.8 sec. In some tests, the preburn time before the blast arrival is noted. Barriers located upstream of the pool are also

studied in some tests. The observations included noting whether or not a given fire is extinguished by a given blast.

Fires of typical wood cribs made of (mostly) dry western hemlock and (some redwood are subjected to overpressures in the range 0.91 to 9.88 psi with postive phases between 0.078-0.117 sec. The cribs are made of sticks either 3/8" or 3/4" thick. A tray of propyl alcohol under the crib is used to prompt the crib ignition following which the crib is allowed to burn for anywhere from about 60 to 180 sec before the blast wave is imposed on the fire.

There are also reported eleven tests in which trays of shredded blotter or filter paper act as fuel beds.

In an attempt to identify the mechanisms of interaction between a fire and a blast, Kanury [5] developed a preliminary scaling analysis in which the physics and chemistry of combustion, as perturbed by the blast effects, come to interplay and decide the fate of the fire. The blast brings with it a rise in pressure and temperature as well as winds. While the pressure and temperature exert an influence on the oxidation reaction rate in a more or less direct way, the air flow exerts a more complicated influence on both the chemistry and physics. Enhanced convection dilutes the reactant mixture thermally as well as compositionally. Reduction in temperature is the consequence of thermal dilution. Increase in the concentration of oxygen (of air) is the result of the compositional dilution. These dilutions directly reflect in conditions conducive to the extinguishment of a flame (namely, the gas-phase oxidation reaction). However, when the fuel bed is constituted of such materials as wood whose char may undergo glowing combustion, the augmented oxygen supply tends to augment the combustion intensity. (This phenomenon is quite familiar to all every-day combustion experimentalists who play with the barbeque charcoal grills.) The outcome of these physico-chemical interactions of the blast with the fire is: (a) the blast, if sufficiently strong, would blow away the flames; and (b) it would exasperate the glowing process. In fact, if the augmentation of glowing is sufficiently large, the glowing objects would support reflashing of a flame upon subsidence of the blast effects. Based on a scrutiny of this interplay between physical transport processes and chemical kinetic reaction processes, Kanury [6] identifies a Damkohler number  $P$  to represent the inverse of the blast strength and a fire strength parameter  $q$  which defines the energeticity of the fire. The definitions of these two scaling parameters are

as following:

$$\text{Inverse blast strength} \quad P \equiv k_0 \ell / u \quad (7.1)$$

$$\text{Fire strength} \quad q \equiv R h_c Y_{F1} / E C_{pg} \quad (7.2)$$

$k_0$  is the preexponential factor of an assumed first-order, overall oxidation reaction,  $\ell$  is the fuel bed characteristic dimension and  $u$  is the maximum

velocity of wind induced by the blast wave.  $R$  is the universal gas constant,  $h_c$  is enthalpy of combustion,  $Y_{F1}$  is the fuel mass fraction at the surface,  $E$  is the activation energy of the oxidation reaction and  $C_{pg}$  is the gas-phase specific heat. As given,  $P$  is a Damkohler number, the ratio of chemical to physical speed.  $u$  will depend upon the pressure as perturbed by the blast.

On a map of  $P(q)$ , regimes in which extinction is expected are distinguished from those in which the fire will sustain the impact of the blast. Where charring fuels are involved, the role of glowing combustion in the reflash of an extinguished flame is examined. The following conclusions, which are reasonably well-founded by the SRI experimental observations, are reached.

(a) Flames, on both liquid and solid fuels, appear to be blown out by the same mechanism.

(b) The  $P$  required to achieve extinction is lower for flames of higher  $q$ .

(c) The influence of an upstream barricade is shown to render the liquid fuel flames more blast-resistant so that the nonextinction region of the  $P(q)$  map is increased. No distinct boundaries, however, can now be drawn for this barricade effect. Experiments are required in which taller barricades are systematically tested. Theory describing the mechanisms of flame stabilization by recirculation has to be developed to compare with these experiments.

(d) The enthalpy of combustion of the fuel, fuel bed length, barricades and shock wave strength are the most important variables in the blast/class B fire interaction process. The fuel vaporization thermodynamics, including enthalpy of vaporization, the nature of wick holding the fuel in the pool, and combustion kinetic parameters appear to have little or no effect on the

response of class B fires to blasts. This is a significant point since such properties as those pertaining to global oxidation kinetics can not be expected to be known in reliable and quantitative detail ever.

(e) The hypothesis of blast/fire interaction postulated and tested with pool fire data is capable of describing fire extinguishment viewed in different ways. for instance, if extinguishment is defined as annihilation of the flame it includes both the degeneration of a stationary flame and 'nonreappearance' of a displaced flame. The flame displacement mechanism advocated by the SRI group thus is completely consistent with the hypothesis.

(f) Having correlated the 12 to 36 inch long liquid pool fire in Ref. [5], the next task in studying class B fires is to develop ways of scaling the fires up to several tens or hundreds of feet in size. Development of these scaling rules requires consideration of such additional factors as : thermal radiation feed-back from the larger flames to the fuel surface, effect of the size of the flames on the uniformity with which the blast would perturb them, accentuation of the recirculation phenomena, and others. Based on the definition of  $P$ , the critical fuel bed length is nearly proportional to the peak over pressure and the particle velocity. This conclusion is similar to that reached earlier by Backovsky et al in Ref. [13].

(g) Turning to class A fires as represented by cribs of wood sticks, it is noted that the mechanisms of flame extinction appears to be the same as that of class B fires. The extinguished state, however, involves charcoal embers capable of undergoing a metastable glowing combustion process. This glowing combustion process supplies sufficient energy to the solid to continue production of pyrolyzates. As the blast effects subside, the cooling (and yet pyrolyzing) embers may pass through a thermochemical state corresponding to reflashing of flame in the mixture of pyrolyzate and air.

Based on the knowledge of the composition of pyrolysis products, and of the relative independence of the extinction boundary of class B fires on the specific nature of the fuel, there seems to be no compelling reason to believe that the flame extinction boundary for crib fires will be different from that for class B fires. The correlation of  $P$  versus  $q$  confirms this idea although this correlation is not as clear-cut as that of liquid fuel flames. The reasons for this can be any combination of such complications as the following. (i) Although it appears logical to expect the preburn time to be an indirect measure of the fire strength  $q$ , the exact connection is not clear

at present. Further study is required of this issue to establish the role of transient conduction (with pyrolysis) in rendering persistence and strength to a crib fire. (ii) In a crib, opportunity exists for the flames to find intense recirculation zones behind individual sticks. These recirculation zones are more effective if the sticks are thicker. Because recirculation tends to stabilize the flames and thus to shift the extinction boundary, it is reasonable to expect nonextinctions where extinction would be expected in the absence of recirculation. The future study recommended above, of flame stabilization by recirculation, will aid in understanding the effect of stick thickness on extinction. The high surface temperature of the wood sticks in a crib will be an important additional parameter to be considered in this connection. (iii) The surfaces at different locations in the crib would char nonuniformly in all crib fires. The distribution of glowing patches which may expediently pilot the reignition of blown-out flames is thus a serious ambiguity of all crib fires. Resolution of this ambiguity requires further work. (iv) Compared to liquid pools, the crib fuel beds are volumetric by two different counts, first by the crib structure itself and second by the conduction-controlled interior of the individual sticks. While the flames over pools are all-important in determining the pool burning rate, the flame over the crib (i.e., the 'top-flame') is of little or no significance compared to the flames within the crib. (v) Thermal radiation from the flames to the fuel surface is more or less unimportant in the class B fires in the size range tested. In contrast, thermal radiation plays a dominant role in the life, strength and death of a crib fire. Additional study is required to gain a better understanding of this role.

The data correlations of Ref. [5] also point out the possibility that the basic burning process of shredded paper fuel beds may be altogether different from that of cribs. It may be closer to that of liquid fuels, but this is yet to be examined by additional study.

(h) The flame reflashing mechanism postulated in Ref. [5] can not at present be tested. It is surprising, however, to note how few experiments in the SRI collection in fact show a distinct reflashing. In as much of charcoal glowing is expected to play an important role in this reflashing process, it appears important that a detailed study be undertaken of the effect of blast on glowing wood surfaces. The nature of glowing as it is disturbed by the

last variables, the implications in continued pyrolysis, and possible transition of glowing to flaming, are not only important in understanding the reflashing process but also exciting from the view-point of science.

(i) Turning to scaling, notwithstanding the complicated nature of wood crib fire burning discussed above, crib fires are probably easier to be scaled up since their burning is, more or less, locally controlled. Oxygen depletion in the depths of the crib may, however, become a crucial factor in such scaling endeavors. Thermal radiation effects, of course, are critically required. One important conclusion of the present study is that wood crib burning with and without blast interaction requires much further study before results useful in efforts of mitigation can be obtained.

(j) Shredded paper tray fires are in a class all by themselves in their behavior unexplained at present.

The conclusion one can reach from this status report is that while some preliminary aspects of blast/fire interaction have been studied to date, much remains to be done. The blast strength parameter  $P$ , fire strength parameter  $q$ , and barricade height (ratioed with the fuel bed length) appear to be the predominant scale variables. Shredded paper tray fires are altogether poorly understood as to their response to an imposed blast wave. Lastly, little is known of the response of vertical fuel bed fires and of the role played by thermal radiation--both from the thermal pulse residual and from the fire itself. Multiple blast effects and multiple fire effects are also yet to be studied.

## SECTION 8

### FIRE PROPAGATION AND GROWTH

Born of the impingement of the thermal pulse on combustibles and perturbed in its infancy by the arrival of the blast wave with its attendant rise in pressure, temperature and wind, the fire finds for its survival a scenario of disturbed objects amidst piles of debris. The same blast which caused mechanical disruption of bodies to generate the debris, also brings about the secondary fires. Notwithstanding the fact that combustibles and noncombustibles are randomly mixed to form the debris piles, these piles are expected to offer an effective base upon which both the secondary fires and the blast-survived primary fires flourish. A combination of both smoldering and flaming fires is foreseeable. Since the fires are expected to continue burning for days (or even weeks) after the blast, they pose a continued (and growing) hazard which can be either further aggravated or brought under control.

Fire growth is a topic of extensive scientific study. The mechanisms of flame spread on contiguous fuel beds in small scale have been thoroughly reviewed by F. A. Williams [15]. The relatively better definable and controllable configurations of downward flame spread (on vertical combustible surfaces) and horizontal spread (on vertical or horizontal surfaces) have been studied most rigorously. The primary conclusion arrived in these studies relates to the mechanism of heat transfer from the 'burning' zone to the fuel yet to be involved. Conduction through the gas phase, through the solid phase, convection in the gas phase, convection in the condensed phase (in liquids) and thermal radiation are among the identified heat transfer mechanisms. While these studies are useful in understanding the fundamental processes of fire growth, they are less relevant in practice than situations involving: (a) spread of fire by a smolder front; (b) horizontal and downward flame spread in opposing wind; (c) upward fire spread on vertical surfaces; (d) fire spread in a forest; (e) radiant heating and jumping fire spread in discrete fuel elements; and (f) growth in compartments.

8.1 Spread of a Fire by a Smolder Front: A nonflaming exothermic oxidation reaction wave propagating within a porous combustible solid medium constitutes smolder. As energy is released at the smolder front, part of it is lost, predominantly by conduction, through the solid to the surroundings

while the rest is employed to preheat the solid to the state of smoldering. Ohlemiller and Rogers [16] propose that if the balance between energy generation and loss were to be the controlling factor in determining a sustained smolder spread, then the energetics, transport properties and kinetics of smolder reactions have to be such that a nondimensional parameter  $\delta$ , defined below, has to exceed a certain minimum value.

$$\delta = \frac{h_c Z E \ell^2 \exp(-E/RT_p)}{K R T_p^2} \quad (8.1)$$

The larger the heat loss (expressed as a Biot number defined below), the larger the minimum value of  $\delta$ .

$$Bi = \frac{h \ell}{K} \quad (8.2)$$

$h_c$  is heat of combustion of the smolder reaction whose preexponential factor is  $Z$  and activation energy is  $E$ .  $R$  is gas constant.  $T_p$  is smolder temperature.  $\ell$  is half-thickness of the solid whose conductivity is  $K$ . The surface of the solid loses heat to the surrounding by convection,  $h$  being the corresponding heat transfer coefficient. A high ambient temperature  $T_\infty$  nondimensionalized as  $\theta_\infty = E(T_\infty - T_p)/RT_p^2$  causes the critical  $\delta$  to be smaller. In contrast, Palmer [17] and other workers invoke the rate of oxygen transfer through the porous layer as a governing factor of the smoldering rate. Two situations can be envisioned. In the first, the smolder wave propagates into the material from near the surface exposed to the environment. In this case, oxygen diffusion has to occur through the residual 'char' to the propagating front. Since the char thickness offers a gradually increasing resistance to oxygen diffusion, the smolder speed decreases as the inverse square-root of time and hence the smoldered thickness varies as  $\sqrt{t}$ . In the



second, the smolder propagates from within the fuel bed towards the exposed surface, thus encountering progressively smaller diffusion resistance to the oxygen supply. Although a  $\sqrt{t}$  dependency arises again (as characteristic of all diffusion problems), the spread speed increases with time in this situation. The smolder spread history thus appears to be scaleable in terms of the dependent parameter  $V$  and independent parameter  $D$  defined below.

$$V = \frac{(\rho_s - \rho_c) u \ell_s C_{ps}}{K_s} \quad (8.3)$$

$$\hat{D} = \frac{\rho_g D Y_{O_\infty} t}{f(\rho_s - \rho_c) \ell_s^2} \quad (8.4)$$

where  $\rho_s$  and  $\rho_c$  respectively are the initial and final density of the solid;  $\rho_g$  is the ambient gas (i.e., air) density;  $\ell_s$  is the physical characteristic thickness of the smoldering solid of specific heat  $C_{ps}$  and conductivity  $K_s$ ;  $D$  is diffusivity of  $O_2$  through the char or the original solid depending upon the spread direction,  $Y_{O_\infty}$  is the ambient oxygen mass fraction (normally 0.23), and  $f$  is the stoichiometric mass ratio of fuel to oxygen.  $u$  is spread speed and  $t$  is time.

The state-of-the-art of smolder spread is still in its infancy. Detailed scaling rules are yet to evolve, especially when thermal radiative heat transfer within the porous fuel bed assumes the controlling responsibility for the spread process.

8.2 Horizontal and Downward Flame Spread in Opposing Wind: As a prelude to the problems of more direct concern in the context of this report, we shall review here but briefly the salient current understanding of the wind-opposed fire spread. The literature abounds with reports on the mechanism of this fire spread process.

de Ris [18] presented a landmark analysis of fire spread on a horizontal fuel bed (thin and thick) in opposed oxidant flow to bring the first orderly

quantitative interpretation of all the then existing flame spread information. The primary accomplishment of this work is the derivation of

$$\frac{\rho_s C_{ps} \ell_s u (T_{vap} - T_{\infty})}{\sqrt{2} K_g (T_f - T_{vap})} \approx 1 \quad (8.5)$$

for thin fuels of thickness  $\ell_s$ . The evaporating surface temperature  $T_{vap}$  is representative of the evaporation thermodynamics or pyrolytic decomposition.  $T_g$  is the temperature of the spreading flame.  $T_{\infty}$  is temperature of the ambient gas whose conductivity is  $K_g$ . For thick fuel beds, the following prediction is made.

$$\frac{\rho_s C_{ps} K_{sy} u}{\rho_g C_{pg} K_g u_g} = \left\{ \frac{T_f - T_{vap}}{T_{vap} - T_{\infty}} + \frac{2R_1 F(z) + 2R_2/\pi}{\rho_g C_{pg} u_g (T_{vap} - T_{\infty})} \right\}^2 \quad (8.6)$$

where subscript g stands for the gas phase,  $u_g$  is the velocity of opposing wind flow,  $R_1$  and  $R_2$  are upstream and downstream radiative heat fluxes, and  $F(z)$  is a given function of

$$z \equiv \frac{2K_g}{\rho_g C_{pg} u_g \ell_1} \quad (8.7)$$

where  $\ell_1$  is the characteristic length of the forward radiation.

These remarkable relations vividly point out the manner in which various properties, conditions and variables combine to form the scale parameters for the phenomenon of laminar horizontal diffusion flame spread.

F. A. Williams [15] pulled together the various mechanisms of fire spread over condensed-phase combustibles into a coherent framework based on the following nondimensional rendition of the classical concept of Mallard and Le Chatelier.

$$\frac{\rho_s u \Delta h_s}{\dot{q}''} = 1 \quad (8.8)$$

Here,  $\rho_s$  is the fuel density,  $u$  is fire spread velocity,  $\dot{q}''$  is the rate of heat transfer across the surface (or line) of fire inception and  $\Delta h_s$  is the rise in fuel enthalpy required to bring the supply fuel to the ignition state.

The heat flux  $\dot{q}''$  depends upon the specific mechanism of heat transfer which drives the flame spread process. If it is the solid-phase conduction, then  $\dot{q}'' \approx K_s(T_{\text{vap}} - T_\infty)/\lambda_s$  where  $\lambda_s$  is the conduction characteristic length. It is thus evident that  $\rho_s u \Delta h_s \lambda_s / K_s(T_{\text{vap}} - T_\infty) \approx 1$  becomes the scaling prescription in this situation. When  $\Delta h_s$  can be written as a product of specific heat  $C_{ps}$  and temperature rise, this prescription further reduces to a Peclet number criterion, viz:  $u \lambda_s / \alpha_s \approx 1$  where  $\alpha_s = K_s / \rho_s C_{ps}$  is thermal diffusivity. The conduction length  $\lambda_s$  itself may either be a geometric parameter such as the fuel element thickness or be a transient parameter, i.e.,  $\lambda_s \approx \sqrt{\alpha_s t}$ , where  $t$  is time.

If conduction in the gas phase were to be operative, the heat flux is given by  $\dot{q}'' = h(T_f - T_{\text{vap}})$  so that  $\rho_s u \Delta h_s / h(T_f - T_{\text{vap}}) \approx 1$  constitutes the scaling restraint. Denoting the gas phase conduction length by  $\lambda_g$ , it is noted that  $h \approx K_g / \lambda_g$  where  $K_g$  is the gas phase conductivity so that one can arrive at the alternate scaling law  $\rho_s u \Delta h_s \lambda_g / K_g(T_f - T_{\text{vap}}) \approx 1$ . For a thermally thin fuel element,  $\lambda_g$  may be expected to be of the same order of magnitude as  $\lambda_s$  so that the present results are consistent with the result of de Ris.

Let  $\lambda_s$  be the depth to which a thick solid (of density  $\rho_s$ , specific heat  $C_{ps}$  and conductivity  $K_s$ ) required to be heated (from  $T_\infty$  to  $T_{\text{vap}}$ ) in order to receive the leading edge of the flame spreading at a speed of  $u$ . Then the energy demand, per unit width of the solid, is given by  $\rho_s u C_{ps} \lambda_s (T_{\text{vap}} - T_\infty)$  Watts per meter. The energy supply rate, per unit width, from the flame to the solid at the leading edge is  $\dot{q}''_g \lambda_g$  (W/m) where the heat flux  $\dot{q}''_g$  will be further discussed later; and the characteristic gas phase length is  $\lambda_g$ . The ratio of demand to supply constitutes a dimensionless ratio of importance in the spread process. This ratio is  $\rho_s C_{ps} u \lambda_s (T_{\text{vap}} - T_\infty) / \dot{q}''_g \lambda_g$ . The

perturbed solid depth can be expected to be of the order of  $K_s(T_{vap} - T_\infty)/\dot{q}_g''$ . The heat flux  $\dot{q}_g''$  is transmitted forward in the gas phase to heat the solid. If  $u_g$  is the opposing gas flow velocity, the forward transmission is described by a Stanton number similarity mechanism so that  $\dot{q}_g'' = \rho_g u_g C_{pg}(T_f - T_{vap})$ . Its delivery to the solid in the vicinity of the leading edge is described by the essential relation  $\dot{q}_g'' \sim K_g(T_f - T_{vap})/\ell_g$ . Substitution of these relations into the demand/supply ratio governing the spread process leads to

$$\frac{\rho_s C_{ps} K_s u (T_{vap} - T_\infty)^2}{\rho_g C_{pg} K_g u_g (T_f - T_{vap})^2} \sim 1. \quad (8.9)$$

This relation is identical to de Ris' thick body result in the absence of radiation.

8.3 Upward Fire Spread on Vertical Surfaces: This problem of practical importance is characterized primarily by the fact that the gravitationally induced hot gas flow is in the same direction as the flame spread. As a consequence of the enhanced heat transfer to the upstream fuel which is yet to be involved in the upward spreading flame, the flame spread rate is higher. It is evident from practical observation that as the fire grows progressively larger, its growth rate also progressively increases as prompted by the progressively greater heating. Estimations of this accelerative growth places it between an exponential ( $\exp t$ ) to a power law ( $t^n$ ) type time-functions for the flame spread rate.

While the mechanism of upward spread rate is qualitatively known from practical observations, the available scientific analysis of this problem is relatively limited. Pello [19] reports an analysis of upward laminar fire spread while Orloff et al [20] report on certain turbulent fire spread studies. Pello's analysis points out that while the thermodynamic aspects of the problem are describable by the Stefan number  $C_{pg}T_{g\infty}/L$  and Spalding's B-number  $[f Y_{O\infty} h_c + C_{pg}(T_s - T_\infty)]/L$ , the fluid mechanical aspects are governed by the parameters

$$G = \frac{g x_b^3}{v_{g\infty}^2} \quad (8.10)$$

$$V = \frac{\rho_s C_{ps} u \ell}{K_{g\infty}} \quad (8.11)$$

where  $L$  is (J/kg) is the latent heat of pyrolysis of the solid,  $f$  is stoichiometric fuel/oxygen mass ratio,  $Y_{O\infty}$  is oxygen mass fraction in the ambient air,  $T_s$  is vaporizing surface temperature (same as  $T_{vap}$  in de Ris' results),  $g$  is acceleration due to gravity,  $x_b$  is the length of the fuel surface between the pyrolysis and burn-out stations,  $\nu_{g\infty}$  is ambient gas kinematic viscosity,  $u$  is rate of spread of the pyrolysis front and  $x$  is distance from the origin fixed at the original ignition point.

Sibulkin and Kim [21] performed an analysis in which a parameter  $\phi = \dot{q}'_F / \dot{m}'_f h_c$  is defined with  $\dot{q}'_F$  representing the energy transfer rate per unit width of the upstream uninvolved fuel bed and  $\dot{m}'_f$  is the pyrolyzate mass flow rate per unit width. Gravity enters into both these quantities. If  $\phi$  exceeds a critical value of  $C_{ps}(T_p - T_\infty)/h_c$ , the flame spread rate is unsteady, accelerative. In the steady spread regime, the following relation is deduced.

$$\frac{\rho_s C_{ps} K_s (T_p - T_\infty)^2 u_p}{\dot{q}'_c(x_p) \dot{q}''(x_p)} = \frac{\phi}{(4/3)^j} \quad (8.12)$$

$j = 1$  for laminar spread and  $j = 0$  for turbulent spread.  $\dot{q}'_c = \dot{m}'_f h_c$  is the combustive heat release rate (W/m) per unit width of the fuel plate. ( $\dot{m}'_f$  is the fuel production rate per unit width.)  $\dot{q}''(x_p)$  is the energy feedback rate (W/m<sup>2</sup>) at the pyrolysis front  $x = x_p$ . This flux is relatable to the pyrolysis rate  $\dot{m}$  at  $x = x_p$  through the latent heat of vaporization  $L$  as  $\dot{q}''(x_p) = \dot{m}''(x_p) xL$ . The nondimensional flame spread velocity parameter on the left-hand side of the foregoing relation bears a remarkably close similarity with that derived in the preceeding section for horizontal wind-opposed flame spread.

It is thus evident that although the focus of the existing works on the upward flame spread problems is predominantly on the involved mechanisms, certain scaling relations can be deduced from their basis. It must be noted however, that when large scale fires are of concern, thermal radiation effects come into play profoundly and can not easily be incorporated in the existing framework of knowledge.

8.4 Fire Spread in a Forest: Many attempts have been made to model the problem of fire spread in a forest. Some salient steps of progress will be discussed here to adapt their results for the subject scaling endeavors.

Vogel and F. A. Williams [22] experimented with fire spread across a linear discrete array of vertically oriented match sticks in which the scale is so small as to make convective heating more important than radiative heating. If the fuel elements are thick and their spacing is small, the flame jumps from one element to the adjacent one in a time much shorter than the characteristic conduction time of the solid. Thus solving the element conduction equation with a convective boundary condition, the time to ignition of adjacent stick is obtained. Denoting the stick spacing by  $s$  and ignition time by  $t_i$ , the average fire spread rate  $u = s/t_i$ . The result of Vogel and Williams can then be recast into the form

$$\frac{u(s - y^*)^2}{\alpha_s s} = \frac{4}{\pi} \left\{ \frac{K_g (T_g - T_o)}{K_s (T_i - T_o)} \right\}^2 \quad (8.13)$$

where  $y^*$  is the flame standoff distance on the burning element (so that  $(s - y^*)$  is the distance between the flame and the next ignited stick),  $\alpha_s$  is the stick thermal diffusivity ( $\alpha_s = K_s/\rho_s C_p$ ),  $K$  is thermal conductivity (subscript  $g$  for gas and  $s$  for the fuel solid),  $T_g$  is hot combustion gas temperature,  $T_o$  is initial temperature, and  $T_i$  is temperature of the solid surface at the instant of inception of its flaming. The quantity  $y^*$  depends upon the stick height  $l$  as  $y^* \propto l^n$  where  $n = 1/4$  for laminar flames and  $n \approx 0$  for turbulent flames.

If the stick burnout time  $t_b$  is smaller than the time to ignition  $t_i$  of the adjacent stick, Vogel and Williams expect that the fire would cease to spread. It is observed experimentally that a particular stick ignites at its top and the flame spreads downward at a speed of  $r$  cm/sec. The stick is generally noted to be consumed by the time the flame reaches near the bottom. Thus, Vogel draws  $t_b \approx l/r$ . Thus the fire spread is expected to cease if

$$\frac{\alpha_s l}{r(s - y^*)^2} < \frac{\pi}{4} \left\{ \frac{K_s (T_i - T_o)}{K_g (T_g - T_o)} \right\}^2 \quad (8.14)$$

The rate of downward spread may be obtained by the results discussed in the

preceeding section. That is

$$r = \frac{K_g^2}{\lambda_g K_s \rho_s C_s} \left\{ \frac{T_f - T_o}{T_{ig} - T_o} \right\}^2 \quad (8.15)$$

where  $\lambda_g$  is the gas phase conduction characteristic length which is of the same order of magnitude as the combustible mixture quenching distance.

Substitution gives the condition for ceased fire spread as

$$\frac{\lambda}{s} = \frac{(s - y^*)^2}{s \lambda_g} \frac{\pi}{4} \left\{ \frac{T_f - T_o}{T_{ig} - T_o} \right\}^2 \quad (8.16)$$

The temperature ratio appearing on the right-hand side of this criterion relation is expected to be larger than unity but only slightly. Recalling that  $y^* \propto \lambda^n$  and that a combustible mixture of high energetic intensity and reactivity will exhibit a smaller quenching distance  $\lambda_g$ , it is clear from the given relation that short fuel elements spaced further will fail to support a spreading fire.

Emmons and Shen [23] studied the horizontal fire spread over a fuel bed made of paper strips of height  $H$  placed parallel to one another at a spacing of  $S$ . The flame spread rate  $u$  along the strips has been nondimensionalized with the paper thickness  $\tau$ , paper density  $\rho$  and conductivity  $K$ .

$$V = \frac{u \rho C_p \tau}{K} \quad (3.17)$$

This has been shown to depend upon the ratio of strip height to spacing ratio  $H/S$ . When  $H/S < 2$ , laminar flames are observed (with their height  $L_f \propto u \rho H$ ) and when  $H/S > 2$ , turbulent flames are noticed ( $L_f \propto (uH/g^{1/2}S)^{2/3}$ , where  $g$  is acceleration due to gravity. Furthermore, the flames on adjacent paper strips would merge if the spacing is small, i.e., if  $S < 0.4 + 0.26 H$  with  $S$  and  $H$  in cm.

While Vogel's study accounts for only convective heat transfer from the hot flame gases to the element yet to be ignited, Shen's study accounts for radiant heat transfer from the embers, convective heat transfer from the flame gases and radiative heating from the flames with an assumed flame height correlation.

Atallah [24] proposed a forest fire model involving radiation to arrive at the following result

$$A = \frac{2D(B+C)}{[4(B+C) - D]} - \frac{4(B+C)}{D} + 1 \quad (8.18)$$

where A, B, C and D are scaled variables defined below.

$$A = \frac{uH}{\alpha_s} \quad \text{fire spread velocity} \quad (8.19)$$

$$B = \frac{\bar{h}H^2}{K_s \tau} \quad \text{convective loss} \quad (8.20)$$

$$C = \frac{\sigma \epsilon_s H^2 (T_p^4 - T_\infty^4)}{K_s \tau (T_p - T_\infty)} \quad \text{reradiant loss} \quad (8.21)$$

$$D = \frac{\sigma \epsilon_s \epsilon_f H^2 (T_f^4 - T_\infty^4)}{K_s \tau (T_p - T_\infty)} \quad \text{radiant heating.} \quad (8.22)$$

H here is the height of the flame.  $\alpha_s$  and  $K_s$  are respectively the thermal diffusivity and conductivity of the fuel bed whose thickness is  $\tau$ .  $\bar{h}$  is convective heat loss coefficient between the preheating fuel and the surroundings.  $\epsilon_s$  and  $\epsilon_f$  are the emissivities of the fuel bed and the flame.  $\sigma$  is Stefan-Boltzmann Constant.  $T_\infty$ ,  $T_p$  and  $T_f$  are temperatures respectively of the surroundings, the pyrolyzing fuel and the flame.

The flame height H in this scaling argument is yet an unscaled dependent parameter. In order to obtain this scaling, we resort to the available flame height analyses as following.

The inlet momentum of the fuel supply in buoyant flames is extremely small; the momentum produced by buoyancy becomes the all important issue in determining the size of a flame and the wind-flow induced by it. Thomas [25-27] studied the problem by applying dimensional analysis methods to correlate the experimentally measured heights of turbulent stationary fires.

Thomas argues the height of a turbulent buoyant fire is expectable to depend upon the volumetric fuel feed rate  $\dot{V}$ , for it is a measure of not only



the total quantity of fuel to flow through the plume but also of the amount of air drawn into combustion. Since the velocity induced  $u_g$  in a gravitational field of acceleration  $g$  by a fire of base diameter  $d_0$  has to be of the order of  $\sqrt{g d_0}$  (so that the Froude number  $u_g^2/gd_0$  is preserved), and since  $u_g \sim \dot{V}/d_0^2$ , the flame height  $H$  measured in units of  $d_0$  is expected to depend upon the nondimensional ratio of either  $u_g^2/gd_0$  or  $\dot{V}^2/gd_0^5$ . The source of buoyancy in a fire is the lower density of the fire gases compared to the ambient air. This density difference is mainly a consequence of the high flame temperature. To account for the larger buoyancy produced by hotter fires, therefore, the dimensionless temperature difference  $\beta_v(T_f - T_\infty)$  has to enter the correlation.  $\beta_v$  is the volumetric expansion coefficient ( $1/K$ ) of the fire gases. Since body forces are associated with the gravitational constant, this expansion term enters into the denominator of the Froude number. Thus

$$\frac{H}{d_0} = f_1\left(\frac{\dot{V}^2}{g d_0^5 \beta_v \Delta T}\right) \quad (8.23)$$

The velocity  $u_{tip}$  attained by the buoyantly accelerated flame gases at the flame tip has to be a function of both the flame height and the modified Froude ratio.

$$\frac{u_{tip}}{\sqrt{g x_f}} = f_2\left(\frac{H}{d_0}, \frac{\dot{V}^2}{g d_0^5 \beta_v \Delta T}\right) \quad (8.24)$$

The fuel input rate is sometimes known in terms of mass rate  $\dot{m}_0$  (kg/s) which is related to the volume flow rate  $\dot{V}$  as  $\dot{V} = \dot{m}_0/\rho_0$ . Thus the Froude number in the preceding two equations can take the following form

$$Fr = \frac{\dot{m}_0^2}{\rho_0^2 g d_0^5 \beta_v \Delta T} \quad (8.25)$$

Since the energy release rate  $\dot{Q}$  in the fire can be related to the fuel feed rate  $\dot{m}_0$  through the heat of combustion  $h_c$  as  $\dot{Q} = \dot{m}_0 h_c$ , yet another way of

expressing the Froude number exists.

$$Fr = \frac{\dot{Q}^2}{\rho_0^2 h_c^2 g d_0^5 \beta_V \Delta T} \quad (8.26)$$

Throughout these dimensional deductions, consideration is not given to the fact that the fire fluid elements at different heights in the flame experience different levels of buoyancy. Steward [28,29] analyzed the distributed buoyancy problem to arrive at the following prediction for flame height.

$$\frac{H}{d_0} = 1.49 \left\{ \frac{1}{\pi^2 k^4} \cdot \frac{\dot{Q}^2}{\rho_0^2 h_c^2 g d_0^5} \cdot \left[ \frac{[(rT_\infty/T_0) + \omega]^2}{(1 - \omega)^5} \right] \right\}^{1/5} \quad (8.27)$$

where  $k$  is jet entrainment coefficient ( $\approx 0.10$ ),  $r$  is the stoichiometric air/fuel mass ratio, and  $\omega = T_\infty/(T - T_\infty) = \rho/(\rho_\infty - \rho)$  is the inverse of volumetric expansion due to combustion,  $T$  and  $\rho$  being temperature and density of the flame gases. In addition to being a predictive relation for the heights of stoichiometrically burning buoyant turbulent fires, this equation of Steward retains the basic form of the Froude number given by the earlier equation with only the expansion term spelled out by the function of  $r$  and  $\omega$  square-bracketed above.

The available flame height data when compared to the above prediction indicates that while the predicted 1/5th power dependency is satisfactorily verified, the mixtures existing in real fires are clearly not stoichiometric. Steward estimates that an assumed 400% excess air would make his predictions quite close to the experimental data. Experience with natural fires indicates that this excess air figure is quite expectable.

These stationary fire height correlations might be adaptable to propagating fires if the fire-seat diameter  $d_0$  and the fuel inlet velocity  $(\dot{Q}/h_c + d_0^2 \rho_0)$  can be suitably redefined. Denote the mass of fuel per unit area of the forest floor, that will be burned by the fire sweeping at a speed of  $u$ , by the symbol  $m''$ . Let  $\dot{m}''$  be the average burning rate per unit area. While  $m''(\text{kg}/\text{m}^2)$  is a prescribable fuel-load characteristic of the forest,  $\dot{m}''(\text{kg}/\text{m}^2\text{sec})$  will depend upon the thermochemistry and combustibility of the forest fuel. Then the width  $w$ , of the burning zone of the spreading fire, will be given by  $w = u m''/\dot{m}''$ . This  $w$  is generally expectable to be nearly

linearly proportional to the forest fuel bed height  $\tau$ . It appears reasonable that  $d_0$  in Steward's correlation formula can be replaced by  $w$ . Furthermore, the fuel feed rate  $(\dot{Q}/\rho_0 \pi d_0^2 h_c)$  has obviously to be replaced by  $(\dot{m}''/\rho_0)$ . Upon doing this, the following set of forest fire spread scaling parameters are realized from Atallah's work.

$$\overline{A} = \frac{u m''}{\tau \dot{m}''} \quad \text{fire spread velocity} \quad (8.28)$$

$$\overline{B} = \frac{\overline{h} \tau}{K_s} \quad \text{convective loss} \quad (8.29)$$

$$\overline{C} = \frac{\sigma \epsilon_s (\tau_p^4 - \tau_\infty^4)}{\overline{h} (\tau_p - \tau_\infty)} \quad \text{radiative loss} \quad (8.30)$$

$$\overline{D} = \frac{\sigma \epsilon_s \epsilon_f (\tau_f^4 - \tau_\infty^4)}{\overline{h} (\tau_p - \tau_\infty)} \quad \text{radiative heating} \quad (8.31)$$

$$E = 1.49 \left\{ \frac{1}{k^4} \left( \frac{\dot{m}''}{\rho_0} \right)^2 \frac{1}{g \tau} \left[ \frac{[(r \tau_\infty / \tau_0) + w]^2}{(1 - w)^5} \right] \right\}^{1/5} \quad \text{Plume dynamics} \quad (8.32)$$

$$F = \frac{\tau^2 \dot{m}''}{\alpha_s \dot{m}''} \quad \text{fuel bed structure} \quad (8.33)$$

Emmons [30] presented an illuminating analysis of a radiatively driven forest fire. A fire spread rate parameter  $R$  and a burning characteristic  $P$  are defined as following.

$$R = \frac{\alpha \dot{m}'' u}{\dot{m}''} \quad (8.34)$$

$$P = \frac{\dot{m}'' C_p (T_i - T_0)}{\alpha Q_b} \quad (8.35)$$

The symbols  $u$ ,  $m''$  and  $\dot{m}''$ , as before, respectively stand for the flame spread rate, fuel loading per unit forest area and average burning rate per unit area. These quantities, as before, determine the width of the burning zone,  $w = u m'' / \dot{m}''$ . The factor  $\alpha$  is a descriptor of the structure of the fuel bed, typically a surface to volume ratio, and has units of 1/meter.  $C_p$  is the fuel specific heat;  $T_i$  and  $T_0$  are respectively the ignition and initial temperature of the fuel solid.  $Q_b$  is the radiant emission intensity of the burning zone. If  $\epsilon_b$  is the burning zone emissivity and  $T_b$  is its temperature,  $Q_b$  is given by  $(\sigma \epsilon_b T_b^4 \tau)$  where  $\sigma$  is the Stefan-Boltzmann Constant and  $\tau$  is the forest fuel-bed height.

Emmons shows that only  $P < 1$  presents a spreading flame. As  $P$  decreases from unity to zero, the fire spread rate  $R$  and the fire zone thickness  $w = (R/\alpha)$  increase from zero to a large value. When  $R$  is large,  $R \approx 1/P$ .

Addressing the issue of a firebreak of width  $g$  in a forest of height  $\tau$ , it is deduced that a radiatively driven forest fire spread is curtailed if  $g/\tau \sim R$ . Furthermore, if  $w_i$  is the width of the initial ignition, the fire would grow to sustain and propagate only if  $\alpha w_i > \ln(1 - P)$ . That is, a small  $P$ , indicative of high combustibility of the forest fuel, will support a sustained fire even with a relatively narrow ignition strip. In contrast, if  $P$  is larger (near unity), the fuel is poor in combustibility and the ignition width  $w_i$  may have to be larger than the steady-spreading fire width  $w$  in order to produce a sustained fire.

While Emmons deals with a number of other interesting aspects of the fire development in a forest, it is sufficient for us to note the following scaling parameters suggested by this work for the radiatively controlled forest fire.

$$R = \frac{\alpha m'' u}{\dot{m}''} \quad (8.36)$$

$$P = \frac{\dot{m}'' C_p (T_i - T_0)}{\alpha Q_b} \quad (8.37)$$

$$G = g/\tau \quad (8.38)$$

$$W = \alpha w_i \quad (8.39)$$

The important effect of wind on flames is not explicitly discussed in any of the above-mentioned investigations. A subtle exception to this statement may be Steward's work which shows that the upward buoyancy and the horizontal induced wind inertia conspire to cause a narrowing of the flame at a small height above the fuel source. But more relevantly, Welker, Pipkin and Sliepcevich [31] have studied the bending of pool fires in a cross-wind. Hamada [32] investigated the bending of building fires in cross-wind. Both of these works indicate that the Froude and Reynolds numbers are the primary criteria governing the flame tilt angle. Welker's momentum balance on the flame leads to the result

$$\tan \theta = \frac{K}{2f(1 - \frac{\rho_f}{\rho_a})} \left[ \left( \frac{v^2}{gd} \right)^n / \left( \frac{\rho_a v d}{\mu_a} \right)^m \right] \quad (8.40)$$

where  $\theta$  is tilt from vertical;  $K$  is a constant (near about 60);  $f$  is a flame shape factor (upright cylinder  $f = \pi/4$ ), slab  $f = 1/2$ , cone  $f = \pi/6$ , pyramid  $f = 2/3$ , and parallelepiped  $f = 1$ );  $\rho_f$  and  $\rho_a$  are the densities respectively of the flame gases and ambient air;  $v$  is wind speed;  $g$  is gravity;  $d$  is fire base diameter and  $\mu$  is ambient air dynamic viscosity. The group  $v^2/gd$  is Froude number while  $\rho_a v d / \mu_a$  is Reynolds number. The indices  $n$  and  $m$  are equal to  $1/2$ . Hamada's experiments lead to a similar result with the mere difference that  $n = 1$  and  $m = 0$ .

Welker and Sliepcevich [33] reported that the temperature in the convective plume tilted by the wind can be uniquely correlated in the framework of the following parameters for wide line fires.

$$\phi = \left( \frac{T - T_a}{T_a} \right) \frac{gx}{\left[ \frac{gQ'}{\rho_a C_p T_a} \right]^{2/3}} \quad (8.41)$$

$$\Omega = \frac{v}{\left[ \frac{gQ'}{\rho_a C_p T_a} \right]^{1/3}} \quad ; \quad \xi = \frac{x}{w} \quad ; \quad \zeta = \frac{z}{w} \quad (8.42)$$

where  $T$  is temperature in the plume at a distance  $x$  downstream from the center of the pool,  $T_a$  is ambient temperature and  $Q'$  is total heat output rate of the fire per unit length.  $w$  is width of the fuel pool channel.  $z$  is height from the floor. Attention is drawn to the manner in which the heat release rate defines the characteristic velocity in this context. A recent study by Mudan and Croce [34] also confirms the importance of the Froude number in determining the characteristics of wind-blown pool fires.

Finally, our discussion of forest fire modeling will be incomplete if mention is not made of Rothermel's work [35]. With fuel, weather and topographic parameters measurable in the field as inputs, the model is capable of predicting both the forest fire spread rate and the fire intensity. Keeping consistent with our earlier notation but retaining the British units of the original work, Rothermel's equation for fire spread rate  $u$  (ft/min) is:

$$\frac{\rho_b \epsilon Q_i u}{\dot{m}'' \xi (1 + \phi_w + \phi_s)} = 1 \quad (8.43)$$

where  $\rho_b$  is fuel bulk density (lbm/ft<sup>3</sup>);  $\epsilon$  is an effective heating number ( $\epsilon = \exp(-138/\sigma)$  where  $\sigma$  is fuel particle surface area to volume ratio, 1/ft);  $Q_i$  is energy of preignition (Btu/lbm) ( $Q_i = C_p(T_i - T_0)$ ) in the perspective of our earlier discussions where  $C_p$  is the fuel specific heat,  $T_i$  is its ignition temperature, and  $T_0$  is its initial temperature and  $Q_i = 250 + 1,116 M_f$  for forest fuels of moisture content  $M_f$  lbm of moisture/lbm of oven-dry wood);  $\dot{m}''$  reaction intensity (Btu/ft<sup>2</sup>min) (a function of optimum chemical reaction velocity, net fuel loading, fuel particle heat content, damping of the reaction due to moisture, and damping of the reaction due to mineral content);  $\xi$  is propagation flux ratio (a function of the fuel particle surface to volume ratio and of the fuel packing ratio,  $\beta$ );  $\phi_w$  is wind factor (a function of the wind speed,  $\sigma$ , and  $\beta$ ); and  $\phi_s$  is the slope factor (a function of  $\beta$  and the slope of the terrain). Note that  $\epsilon$ ,  $\xi$ ,  $\phi_w$  and  $\phi_s$  are all nondimensional factors.

Rothermel's work has enjoyed remarkable success in forest fire control. It is interesting to note that the product of Emmons parameters  $P$  and  $R$ ,  $PR = \dot{m}'' C_p(T_i - T_0)u/Q_b$ , shares a remarkably common conceptual basis with

Rothermel's fire spread rate parameter in the form presented above. The main difference is that Rothermel's model goes into much greater detail of the burning zone heat flux  $Q_b$  than does Emmons' model.

8.5 Fire Growth in Compartments: While the previous section has dwelt much on fire spread outside buildings, we deal in this section with the plausibility of scaling the fire growth process within a room. A recent paper by Kanury [4] forms the basis of this discussion although literature is plentiful of investigations on this issue.

As the initial fire burns under conditions of essentially unrestrained air supply, its hot gases and flames convect and radiate energy to the enclosure walls in a manner affected by the fire location/size and the room/ventilation details. Conductive heating of the linings will lead to pyrolysis, vaporization or charring to produce combustible vapors which then convectively mix with air and ignite to enhance the flame volume. The conductively heated walls may emit radiation to make the room a sort of an energy augmentor, an introspective hohlraum. Accumulation of smoke near the ceiling, however, may soon attenuate the surface radiant heat exchange and introduce soot layer radiation into the subsequent heating process. All during this transient process; either, the initial fire is continuously and acceleratively growing towards the state of a physico-chemical catastrophe known as flashover; or, if the initial fire is externally controlled to maintain a constant size/intensity such as could be done with a gas burner, the room wall linings are gradually heated to arrive at a critical thermochemical state at which the various surfaces tend to be simultaneously ignited.

The variables of influence identifiable by this description exhibit nonlinear interactions among the various time-dependent fire processes. The room geometry, for instance, mutilates the thermal radiative exchange of energy in the room as well as alters the convective flows of air and hot gases and the associated mixing and heating phenomena. As a result, the ignition (and/or fire spread) will be influenced by the room geometry.

The ventilation intensity will obviously affect the air supply rate to the fire, convection and mixing, accumulation of smoke in the ceiling layer and hence the overall thermal radiation process itself. Herein arises the important connection between the window geometry (which determines the flow of gases) and the lintel height (which determines the thickness of the hot

ceiling gas layer). The energy balance responsible for continued fire-growth process (or the ignition process of various parts of the room) is thus tampered by the ventilation characteristics.

The nature of the initial fire and its proximity to the lined walls shall result in convective and radiative heating of the adjacent surfaces, thus preparing them towards the thermochemical state of ignition. In this entire picture of heat exchange, the wall linings play not only the active role of confining the gas flows and absorbing/reflecting/emitting thermal radiation but also a passive role of being heated by transient conduction progressively towards a thermochemical state of receiving the growing fire or of spontaneous ignition.

This qualitative discussion leads one to believe that the flashover problem entails two specific questions: (a) Is flashover possible under a given set of conditions of the room geometry, ventilation, initial fire and wall-lining? (b) If it is possible, how does the time to flashover depend upon these prescribed conditions? The answers to these questions require that the experimental fire growth data be represented on the basis of a dimensional analysis of the problem of room fire growth and the associated transient heating of the room. It is apparent that the variables expected to influence the growth of a room fire to flashover pertain to the following five groups:

- a. room geometry -- volume, depth and height, lintel height, etc;
- b. ventilation -- door/window location and dimensions;
- c. fuels -- furnishings and wall linings;
- d. initial fire -- size, location, burning rate, etc; and
- e. heating of walls and ceiling by conduction, convection and radiation.

If the variables involved are thus identified, five independent dimensionless parameters are expected to evolve pertaining to the five families of variables listed above. (For the convenience of this discussion, these parameters will be denoted by A, B, C, D, and E.) Typically then one can represent the time-wise development of the enclosure fire by systematically altering one of the parameters (say, the initial fire parameter) while the other four parameters are kept fixed. A critical value of the altered parameter is expected to exist representing the occurrence of flashover. Beyond the critical value of the parameter, the time to flashover



will depend on the magnitude of the parameter.

Kanury [4] deduces these scaling parameters from the laws of conservation of mass, energy and momentum. Whereas mass and energy equations dominate in the deduction, the momentum equation comes into play only indirectly in determining the various mass fluxes involved. The species equations are not considered; in the estimation of thermal radiation, smoke is taken as a passive variable its generation rate being considered as a property of the fuel ensemble.

The mass conservation requires under quasi-steady state that the mass of air ( $\dot{m}_a$ ) and fuel ( $\dot{m}_v$ ) entering into the control volume around the room be equal to the mass of combustion products leaving the room ( $\dot{m}_g$ ). While  $\dot{m}_v$  will be determined by the initial fire burning characteristics,  $\dot{m}_a$  and  $\dot{m}_g$  mutually adjust to share the window opening for flow according to the well-known Fujita-Kawagoe equations in which the window height  $H_0$  and width  $W_0$ , densities of the combustion product gas and ambient gas, gravitational constant, and the window orifice coefficient appear as prescribed parameters. Coupling these relations with the relation describing the entrainment of induced air into the fire plume to mix and react with the fuel, one obtains a fully posed problem of flow in the room. The solution of this problem yields the scaled airflow rate  $\phi$  as a function of the (prescribed) scaled fuel input rate  $\phi$  and of the window aspect ratio  $\psi$ :  $\phi = \phi(\phi, \psi)$  with the following definitions.

$$\phi = \dot{m}_a / kW_0 H_0^{3/2} \quad (8.44)$$

$$\phi = \dot{m}_v / kW_0 H_0^{3/2} \quad (8.45)$$

$$\psi = W_0 / H_0 \quad (8.46)$$

$k$  is a constant ( $\approx 1.6 \text{ kg/m}^{5/2}\text{s}$ ) composed of the product gas and ambient air densities, the gravitational constant and the window orifice coefficient. The location of the initial fire within the room is an additional issue which exerts a minor influence on the dependency of  $\phi$  on  $\phi$  and  $\psi$ .

The energy released due to (total or partial) combustion of the fuel mass

supply  $\dot{m}_v$  is used in part to raise the enthalpy of gas flow and to heat up the enclosure walls while the remainder is radiated out through the window. (In the preflashover stage of fire growth, all the combustion may be presumed to be contained within the enclosure so that flames do not shoot out of the opening.) The fuel mass flow rate  $\dot{m}_v$  is generally so small that  $\dot{m}_g \approx \dot{m}_a$ . One can ignore the radiative loss through the window for the introspective consideration of fire growth to flashover. The energy received by the enclosure surfaces can be accounted to heat the (thick) linings by transient conduction. Gas phase phenomena could be construed to follow a quasi-steady behavior.

A synthesis of these ideas leads one to arrive at a dependency of the enclosure surface temperature  $\theta_w$  on time  $\tau$ , air flow rate  $\psi$ , fuel feed rate  $\phi$ , ceiling soffit skirt area  $\gamma$ , and the wall-heating characteristic  $\Omega$ . Since  $\phi = \phi(\phi, \psi)$ , thus  $\theta_w = \theta_w(\tau; \phi, \psi, \gamma, \Omega)$ . The temperature of the hot gases near the ceiling  $\theta_g$  also depends on the same parameters in a nearly same functionality. The scaled quantities are defined as follows:

$$\theta_j \equiv \frac{C_{pg}(T_j - T_a)}{h_c}, \quad j = g, w \quad (8.47)$$

$$\tau \equiv H^2 t / K_w \rho_w C_{pw} \quad (8.48)$$

$$\gamma \equiv \bar{A} / W_o H_o \quad (8.49)$$

$$\Omega \equiv \frac{\bar{h}}{k C_{pg} \bar{H}_o^{1/2}} \quad (8.50)$$

Subscripts g and w respectively represent the hot gas and the heated surface. a is for ambient air, o is for the opening. While t is time, T is temperature. K is thermal conductivity. k is window flow constant mentioned earlier.  $\rho$  and  $C_p$  are density and specific heat respectively. W is width and H is height.  $h_c$  is heat of combustion of the fuel.  $\bar{A}$  is the area of the room surface in its upper reaches which will become contacted by the hot smoke

layer;  $\bar{A}$ , thus, will be the ceiling area plus the product of the room-wall-perimeter near the ceiling and the smoke layer depth.  $\bar{h}$  is the combined convective and radiative heat transfer coefficient between the hot gases and the enclosure surfaces exchanging heat with these gases. The radiative component of  $\bar{h}$  is yet to be fully investigated.

If the initial (prompting) fire characterized by  $\phi$  is situated adjacent to a wall, the wall linings are expected to get ignited and to burn so as to result in a time-wise growing prompting fire. The effect of this will be to expediate the flashover. An additional parameter is required to account for this effect. This parameter has to be a measure of the combustibility of the lining material more specifically, of its thermochemical response. If  $h$  is the heat transfer coefficient between the flame gases at temperature  $T_\infty$  and the lining at temperature  $T_w$ ,  $q$  is heat release rate of the lining sample measured upon exposing to an irradiance of  $I$  and  $f$  is the empirical constant ratio of area covered by a flame to its power ( $f \approx 0.02 \text{ m}^2/\text{kW}$ ), then a wall lining thermal response parameter is definable as

$$\beta \equiv f h (T_\infty - T_w) q / I \quad (8.51)$$

This would then be an additional parameter of the room fire flashover scaling problem.

An application of these scaling arguments to the existing room-fire-test-data indicated that the approach is in correct direction although a more explicit account of thermal radiation appears to be necessary as also a more rigorous consideration of the wall-lining combustibility.

8.6 Radiant Heating and Jumping Fire Spread: While a clean separation of the topics of relevance is not completely possible, two important elements of existing knowledge on fire jump across a distance of separation between two buildings will be discussed here.

First, the study of Mudan and Croce [34] shows that the thermal radiation from trench pool fires decays with distance according to the inverse-square-law from a flux exceeding about  $15 \text{ kW/m}^2$  near the edge of the fire to about  $0.5 \text{ kW/m}^2$  at a distance of about 15 pool (hydraulic) diameters.

Second, Margaret Law [36] reported on safe separation distances between buildings to prevent ignition of successive buildings. Given the intensity of radiation emitted by a fire, and the dimensions and distribution of windows and other openings of the burning building, Law shows that it is possible to calculate the distance beyond which the impingent radiant intensity at a point on a vertical facade facing the burning building would be lower than that required to cause ignition of the facade. The problem becomes one of mere geometry such that this critical distance is given by the equality in

$$\sum_{n=1}^N F_{n-f} > I_c/I_o \quad (8.52)$$

where  $F_{n-f}$  is the radiation view factor between the  $n$ th window opening of the burning building which has  $N$  total openings and the target facade  $f$ .  $I_c$  is the critical irradiance below which the facade material can not be ignited ( $I_c \approx 12.5 \text{ kW/m}^2$  for most cellulosic and synthetic organic materials) and  $I_o$  is the emission intensity of the already burning fire ( $I_o \approx 75\text{--}150 \text{ kW/m}^2$  for most building fires depending upon the degree of ventilation to the burning room). Safe distance, then, is such that  $\sum F_{n-f} > 0.075$  to  $0.15$  approximately. Radiation heat transfer literature (for example, Siegel and Howell [37]) abounds with dictionaries of view factors between surfaces of different shapes disposed in different geometries. Of specific interest in the problem of fire jump between buildings is the view factor between a window (usually, rectangular or square) at a given height and a facing large parallel surface of the target facade.

## SECTION 9

### MASS FIRE

As radiant ignition of a spectrum of combustibles occurs, the fire would tend to grow slowly. Soon would arrive the blast wave to extinguish some of these primary fires and to augment others and, most importantly, to mechanically disrupt structures and installations. The degree of this mechanical disruption depends upon the distance from ground-zero, its consequence being two-fold: first, piles of debris will be formed within which the primary fires surviving the blast would continue to grow; and second, secondary fires will be triggered.

The combination of circumstances would aid the fire to spread in a manner elicited in the preceeding chapter. As the total fire becomes large, it is termed a 'mass fire'. A mass fire is said (Alger [38], Parker [39]) to be a fire of such a large magnitude within which individual fires interact and/or merge with one another to produce a buoyant convective flow pattern intense enough to be capable of perturbing the ambient atmosphere. A mass fire which moves with the prevailing wind is usually known as a conflagration while one which burns stationary is termed a firestorm. Fire devils, high winds, and other severe effects are generally associated with a mass fire to result in an enhanced destructiveness of the fire.

In this chapter, we examine the plausibility of scaling mass fires, especially the firestorms. The discussion includes, in the order, the following topics: (a) Dynamics of plumes over 'small' turbulent fires; (b) radiative effects in plumes; (c) induced wind flow; (d) firebrand transport; (e) fire and wind/fire storms; (f) the combustion zone specifics.

9.1 Dynamics of Plumes over 'Small' Turbulent Fires: Priestley and Ball [40] studied in 1954, the topic of continuous convection from an isolated source of heat. The velocity and temperature fields over finite size fires can be deduced from the given results. Let a fire of radius  $R_0$  be the plume-source of vertical velocity  $w_0$  and temperature  $T_0$ . Let its virtual point source lie at  $z = -z_0$  below the actual fuel surface. Let  $R$  be the radius of the plume at any height  $z$  where the axial velocity and temperature (excess over the ambient temperature  $T_\infty$ ) be  $w_{\max}$  and  $(T - T_\infty)_{\max}$ . The radial ( $r$ ) distributions are found to be given by  $w/w_{\max} = (T - T_\infty)/(T_0 - T_\infty) = \exp(-r^2/2R^2)$ . Denote the scaled velocity and temperature by

$$W \equiv \frac{W}{(3gA/2T_{\infty}c^2z_0)^{1/3}} \quad (9.1)$$

$$\theta \equiv \frac{(T - T_{\infty})}{(2T_{\infty}A^2/3gc^4z_0^5)^{1/3}} \quad (9.2)$$

where  $g$  is gravitational acceleration,  $A \equiv R^2 w_{\max}(T - T_{\infty})_{\max}$ , a constant, indicative of the source energy strength and  $c \equiv dR/dz$ , found from the theory to be a constant near 0.1 indicative of the nature of turbulence which describes the entrainment and mixing in the plume. Then the axial velocity  $w_{\max}$  and temperature excess  $\theta_{\max}$  are obtained to vary with height  $z$  according to the following relations:

$$w_{\max} = \left[ \left( \frac{z_0}{z} \right) - (1 - w_0^3) \left( \frac{z_0}{z} \right)^3 \right]^{1/3} \quad (9.3)$$

$$\theta_{\max} = \left( \frac{z_0}{z} \right)^2 / \left[ \left( \frac{z_0}{z} \right) - \left( \frac{z_0}{z} \right)^3 \right]^{1/3} \quad (9.4)$$

When  $w_0$  is less than  $(2/3)^{1/3}$ , the hot gases will accelerate to a velocity  $w = (2^{1/3}/3^{1/2})(1 - w_0^3)^{-1/6}$  at a height of  $z/z_0 = (3(1 - w_0^3))^{1/2}$  and then decelerate as a result of mixing with entrained fluid. If  $w_0 > (2/3)^{1/3}$ , the accelerating stage will be absent and the motion will decelerate through out. At sufficiently large heights, the first terms of the above equations dominate and the solution approaches

$$w_{\max} = (z_0/z)^{1/3} \quad (9.5)$$

$$\theta_{\max} = (z_0/z)^{5/3} \quad (9.6)$$

In a fire,  $w_0$  is insignificantly small so that  $w_{\max} = [(z_0/z) - (z_0/z)^3]^{1/3}$  which yields the highest velocity of  $w = 0.73$  at a height of  $z/z_0 = \sqrt{3}$  corresponding to a  $z/R_0$  of 7.3.

If the atmosphere is stratified, the stratification parameter  $\gamma$  is defined as

$$\gamma \equiv \left[ \frac{3z_0}{2} \left| \frac{dT_\infty}{dz} \right| / (2T_\infty A^2 / 3gc^4 z_0^5)^{1/3} \right]^{1/4}. \quad (9.7)$$

When  $dT_\infty/dz$  is positive, stable stratification is indicated; otherwise, it is unstable stratification. A small range in  $\gamma$  covers a very wide range in the source strength.

Under stable stratification conditions, the hot gases first accelerate (nearly independent of  $\gamma$ ) and then rapidly decelerate to zero velocity at a certain maximum height which is smaller for large values of  $\gamma$ . That is, there then exists a ceiling beyond which the column does not penetrate. The ceiling height is approximately given by  $(z_{\text{ceiling}}/z_0) \approx 1.9/\gamma^{3/2}$ . Under given environmental conditions, the ceiling height will depend on the source strength but, to a fair approximation independent of the source size.

The abrupt decrease in plume velocity as the height approaches the ceiling height is mainly due to a reversal in the plume buoyancy which occurs at an altitude of  $(z/z_0) = (1 + 1.8/\gamma^3)^{1/2}$  or, for small values of  $\gamma$ , at  $z \approx 0.71 z_{\text{ceiling}}$ .

Under unstable stratification conditions, the gases will first accelerate, then decelerate and cool down but finally pick up acceleration to ultimately reach

$$w \approx \frac{1}{z} \left( \frac{g}{T_\infty} \left| \frac{dT_\infty}{dz} \right| \right)^{1/2} z. \quad (9.8)$$

Morton, Taylor and Turner [41] in a classic paper published in 1956 solved the same problem as Priestley and Ball but with a point source. Define the constant of buoyancy injected into the plume.

$$Q \equiv b^2 u_{\text{max}} g (\rho_\infty - \rho)_{\text{max}} / \rho_\infty \quad (9.9)$$

where  $b$  is a measure of the plume thickness (radial location at which the velocity decays to 1/2 of the  $u_{\text{max}}$ ). While  $b$  is proportional to Priestley's  $R$ ,  $(\rho_\infty - \rho)/\rho_\infty$  for an ideal gas mixture is equal to  $(T - T_\infty)/T_\infty$ . Finally,  $Q$  is related to Priestley's  $A$  by  $Q \equiv (2gA/T_\infty)(b/R)^2$ . Also define a mixing coefficient  $\alpha$ , as the ratio of entrainment velocity to the local maximum velocity in the plume, to be related to Priestley's  $c$  via  $\alpha = (5c/6)(b/R)$ .

Morton's solution is

$$b = \frac{6\alpha}{5} z \quad (9.10)$$

$$w_{\max} = \left( \frac{5}{6\alpha} \right) \left( \frac{9\alpha Q}{10} \right)^{1/3} z^{-1/3} \quad (9.11)$$

$$\frac{g(\rho_{\infty} - \rho)_{\max}}{\rho_{\infty}} = \left( \frac{5Q}{6\alpha} \right) \left( \frac{10}{9\alpha Q} \right)^{1/3} z^{-5/3}. \quad (9.12)$$

These relations are essentially same as the far-field solutions of Priestley and Ball.

The measurements of Rouse, Yih and Humphreys [42] indicate that in any cross section, the plume velocity profile differs from the temperature profile according to

$$\frac{w}{w_{\max}} = \exp(-r^2/b^2) \quad (9.13)$$

$$\frac{(T - T_{\infty})}{(T - T_{\infty})_{\max}} = \exp(-r^2/\beta^2 b^2) \quad (9.14)$$

where  $\beta^2$  is an empirical constant equal to 96/71. Using these profiles in the integral equations of mass, momentum and energy conservation, the following results are obtained for the weakly buoyancy plume [43].

$$b = \frac{6\alpha}{5\sqrt{2}} z \quad (9.15)$$

$$w_{\max} = \left( \frac{5}{6\alpha} \right) \left( \frac{18\beta^2}{5} \alpha Q \right)^{1/3} z^{-1/3} \quad (9.16)$$

$$\frac{g(\rho_{\infty} - \rho)_{\max}}{\rho_{\infty}} = \left( \frac{5Q}{6\alpha} \right) \left( \frac{20}{9\beta^2 \alpha Q} \right)^{1/3} z^{-5/3} \quad (9.17)$$

which are again consistent with the results of Morton and the far-field profiles of Priestley except for slight differences in the coefficients. G. I. Taylor [44] succinctly discusses the implications of these scale relations.



The scaling scheme for the plume dynamics thus seems to be in hand with  $b \propto (\alpha z)$ ,  $w_{\max} \propto (Q/\alpha^2 z)^{1/3}$  and  $g\Delta\rho_{\max}/\rho_{\infty} \propto (Q^2/\alpha^4 z^5)^{1/3}$ . If the fire were a line rather than a point source, then these scale relations are:  $b \propto (\alpha z)$ ,  $w_{\max} \propto (Q'/\alpha)^{1/3}$  and  $g\Delta\rho_{\max}/\rho_{\infty} \propto (Q'^2/\alpha^2 z^3)^{1/3}$  where  $Q'$  is buoyancy source strength per unit length of the fire [45].

9.2 Radiative Effects in Plumes: The relations of the preceeding section make scaling possible of the far-field velocity and temperature distributions in plumes over fires when: (i) thermal radiation is absent; and (ii) the flame and ambient temperatures are same in the prototype as in the scale model. Written explicitly in scaling format, those relations are:

$$\frac{wz^{1/3}}{Q^{1/3}} = \left\{ \left( \frac{5}{6\alpha} \right) \left( \frac{18\beta^2\alpha}{5} \right)^{1/3} \right\} \exp \left( - r^2 / \left[ \frac{6\alpha}{5\sqrt{2}} \right]^2 z^2 \right) \quad (9.18)$$

$$g \frac{(T - T_{\infty})}{T_{\infty}} \frac{z^{5/3}}{Q^{2/3}} = \left\{ \left( \frac{5}{6\alpha} \right) \left( \frac{20}{9\beta^2\alpha} \right)^{1/3} \right\} \exp \left( - r^2 / \left[ \frac{6\alpha\beta}{5\sqrt{2}} \right]^2 z^2 \right) \quad (9.19)$$

wherein,  $b/z = 6\alpha/5\sqrt{2} \approx 0.085 \approx$  a constant is already incorporated into these profiles. Note then  $[6\alpha/5\sqrt{2}]^2 \approx 0.0072$  and  $[6\alpha\beta/5\sqrt{2}]^2 \approx 0.0097$ . The preexponential (square-bracketted) constants are about 6.6 and 21.2 respectively for the velocity and temperature. Remember also that the buoyancy source  $Q$  is defined as  $b^2 u_{\max} g(\rho_{\infty} - \rho)_{\max}/\rho_{\infty}$  whose units are  $m^4/s^3$  and is related to the power  $\dot{q}$  of the fire by  $\dot{q} = [\pi\beta^2\rho_{\infty}C_pT_{\infty}/(g(\beta^2 + 1))]Q$ . Further note that the entrainment velocity  $u_e$  at the edge of the plume at any height  $z$  is given, by definition, as  $u_e = \alpha w_{\max}$ . Thus,  $u_e$  scales according to

$$\frac{u_e z^{1/3}}{Q^{1/3}} = \left( \frac{5}{6} \right) \left( \frac{18\beta^2\alpha}{5} \right)^{1/3} \approx 0.66 \quad (9.20)$$

Hottel [46] notes that modeling thermal radiation in this natural convection of the fire plume can be done at two levels of detail: the first is complete modeling accounting for the alteration of the flow field by thermal radiation; the second is partial modeling only of the radiation from the plume to the surroundings with unaltered flow field.

In seeking complete modeling, one attempts to preserve both the convective modeling discussed above and the following ratio of flame/plume radiation to convective heat transfer.

$$\frac{\sigma(T^4 - T_\infty^4)}{\rho_\infty C_p u (T - T_\infty)} \cdot f(\kappa b, \text{shape}) \quad (9.21)$$

$\sigma$  is Stefan-Boltzmann constant and  $\kappa$  is the plume gas absorption coefficient (1/m). The quantity  $\kappa b$  is proportional to the product of atmospheric pressure and the height. If this product were attempted to be preserved,  $Q$  has to be proportional to  $z^{3/2}$  in conflict with the buoyancy distribution modeling requirement of  $Q \propto z^{5/2}$ . Such a preservation also tampers with the convective heat transfer rate term of the denominator of the above equation by calling for  $Q \propto z^3$ , which too is in vivid contrast with nonradiative plume scaling prescriptions. It is thus concluded that complete modeling of radiation in flames/plumes is impossible.

If one then contents oneself with the partial modeling in the second level of detail mentioned above, then one can satisfy the requirement of  $Q \propto z^{5/2}$  if the flame/plume is radiatively opaque.

Murgai [47] investigates the influence of radiative transfer on the structure of the turbulent convective plume. Standard mass, momentum and energy equations are the starting point of the analysis but a radiative heating rate is added to the energy equation. The effect of radiation is to destroy the constancy of the buoyancy content  $Q$  with respect to height. a nondimensional radiation number

$$\phi \equiv \left( \frac{\kappa \sigma T_\infty^3 b_0^{1/2} \rho_\infty^{1/2}}{C_p g^{1/2} (\rho_\infty - \rho)_0^{3/2}} \right) \left( \frac{4 P_\infty^* (3\gamma - 4)/\gamma}{I \alpha^*^{1/2}} \right) \quad (9.22)$$

is defined.  $P_\infty^*$ ,  $\gamma$ ,  $I$  and  $\alpha^*$  are nondimensional and are respectively: the ambient pressure suitably nondimensionalized with a reference pressure, exponent of the adiabatic law, a shape factor and a constant. All the dimensional properties are in the first bracketed ratio:  $\kappa$  is the absorption coefficient (1/m) of the fluid,  $\sigma$  is Stefan-Boltzmann constant ( $\text{W/m}^2\text{K}^4$ ),  $T_\infty$  is ambient temperature (K),  $b_0$  is source radius (m),  $\rho_\infty$  is ambient density ( $\text{kg/m}^3$ ),  $C_p$  is plume fluid specific heat ( $\text{J/kg K}$ ),  $g$  is gravitational force per unit mass ( $\text{m/s}^2$ ), and  $(\rho_\infty - \rho)_0$  is source density defect ( $\text{kg/m}^3$ ). The first bracketed nondimensional term may be interpreted as a ratio of the

characteristic radiant flux  $\sigma T_{\infty}^4$  to a characteristic input convective heat flux  $\rho_{\infty} C_p T_{\infty} [g(\rho_{\infty} - \rho)_0 / (\kappa^2 b_0 \rho_{\infty})]^{1/2}$  times the fractional initial density defect  $(\rho_{\infty} - \rho)_0 / \rho_{\infty}$ . The quantity in the square-bracket of the characteristic convective flux is a velocity.

Murgai sees that when  $\phi$  is very small, an optically thick (i.e., opaque) limiting case arises to reduce the problem to a plume with no internal radiative exchange. This is entirely consistent with Hottel's conclusion. If  $\phi$  is large, however, the plume is optically thin (i.e., transparent) to alter its development. Murgai numerically integrates the conservation equations to obtain the spreading of the plume, and its velocity and temperature distributions. It is found that radiation does not noticeably change the linearity of growth of the plume radius with height. The more intense the radiation, (i.e., the larger the  $\phi$ ), the fatter the plume. This not due to thermal dilution ascribable to the mass addition by entrainment as in a purely convective plume but due to radiative cooling. The consequent loss of buoyancy is quite vivid even with minor ( $\phi = 0.02$ ) radiation. So also is the rapidity with which the upward velocity decays with height.

Another important paper on modeling fire plumes, is that of Morton [48] in which the characteristics of strongly buoyant plumes as well as the effect of radiation on plume dynamics are discussed.

Both the intermediate and lower regions of the plume are generally much hotter and involve strong buoyancy and thermal radiation. Entrainment in the strongly buoyant regime is expected to depend upon the ratio of local mean plume density  $\rho$  to the ambient density  $\rho_{\infty}$  as well as the lateral momentum,  $\rho w^2$ . Thus, remembering that the entrainment velocity  $u$  is equal to  $\alpha \cdot w$ ,  $\alpha = \alpha(\rho/\rho_{\infty}, \rho w^2)$ . Furthermore, as the plume cools down to the weakly buoyant state,  $\alpha \rightarrow \alpha_w$ , the standard entrainment constant for weak plumes. Additionally, the measurements of Ricou and Spalding suggest  $\alpha \propto \rho^{1/2}$ . These fragments of information led Morton to dimensionally reason that the most viable as well as convenient relation is  $\alpha = (\rho/\rho_{\infty})^{1/2} \alpha_w$ . This is consistent with the common observation that strongly buoyant plumes entrain significantly less than the weak ones; and, as a result, strong plumes spread less rapidly than the weak.

Near-field plume dynamics involve several closely coupled phenomena. For example, the reduced entrainment may significantly influence the combustion process itself which in turn effects the rate of energy and hence buoyancy

injection into the plume. (The fuel pyrolysis and combustion near the source are extremely complex to be incorporated into a realistic scaling scheme; see the work of Nielsen and Tao [49].) Radiation is important in a number of ways. When the absorption coefficient  $\kappa$  is small, (i.e., the radiation mean free path  $1/\kappa$  is large compared to the source size), the plume is transparent. Otherwise, it is opaque; then the vertical flux of radiation  $F$  within the opaque plume core is related to local 'uniform' temperature  $T$  through  $4\pi\sigma dT^4/dx = -3\kappa F$ . Morton nondimensionalizes the problem to realize the following three scaling ratios.

$$A \equiv 8\pi \alpha_w^2 / 3\kappa b_0 \quad (9.23)$$

$$D \equiv \beta g \sigma T_0^4 b_0 / 2 \alpha_w^2 \rho_\infty C_p w_0^3 \quad (9.24)$$

$$C \equiv 2 \alpha_w w_0^2 / g b_0 \quad (9.25)$$

where  $\alpha_w$  is the weak plume entrainment coefficient ( $\approx 0.1$ ),  $\kappa$  is absorption coefficient,  $\beta$  is coefficient of gas expansion, and subscript  $o$  pertains to the source conditions.  $A$  is a measure of the radiation mean free path length to the fire base radius. For opaque flames,  $A$  lies in the range of  $10^{-2}$  to  $10^{-4}$ , so small as to permit ignoring the vertical diffusion of radiation.  $D$  is a measure of the radiative loss to the surroundings relative to the convective energy transport in the plume. Nominally,  $D < 1$ . As the fuel feed velocity gets smaller and the fire base size gets larger,  $D$  increases significantly indicating the dominance of radiant energy loss. The parameter  $C$ , evidently, is a modified Froude number,  $\approx 1$ . Morton, thus, appears to cover the important problem of opaque strongly buoyant plume in distinct contrast with, and dramatic complement to, the transparent weakly buoyant plume scaling suggested by Murgai.

9.3 Induced Wind Flow: Some Estimates and Some Measurements: An examination of the scaling rules developed in section (a) above indicates that the far-field entrainment velocity  $u_e$  depends on height  $z$  above the source of strength  $q$  as

$$\frac{u_e z^{1/3}}{q^{1/3}} \approx \text{constant, near } 0.66 \quad (9.26)$$

The constant itself may be somewhat smaller in the near-field due to the observation of Morton that for strongly buoyant plumes,  $\alpha = (\rho/\rho_\infty)^{1/2} \cdot \alpha_w$ .

Priestley's  $W_{\max} = W_{\max}(W_0, z_0/z)$  relation can be transformed to the following relation for entrainment velocity.

$$\frac{u_e z^{1/3}}{Q^{1/3}} = \left(\frac{25}{24} \alpha\right)^{1/3} \left[1 - \left(\frac{z_0}{z}\right)^2\right]^{1/3} \quad (9.27)$$

Assuming  $\alpha = 0.1$ , the plume spreads with a slope of 0.1 so that for a source of radius  $b_0$ , the virtual source lies at a distance of  $z_0 = 10 \times b_0$  below the real source. While the far-field solution indicates that as  $z \rightarrow z_0$ ,  $u_e$  tends to a large value, the Priestley solution implies that  $u_e(z \rightarrow z_0) \rightarrow 0$  which is physically quite reasonable.

Taylor [44] discusses, in rather general terms, the issue of air inflow into fire plumes to primarily highlight the, now well-known, fact that both the axial velocity  $w$  and lateral (entrainment) velocity  $u_e$  vary with height  $z$  raised to a power of  $-1/3$ . This recognition of the proportionality  $u_e \propto w$ , which is a latent consequence of the involved turbulent mixing mechanism, is indeed profound, for the seed is sown to the eventual development of the concept of entrainment constant.

Faure [50] points out that in the great Hamburg raid, two out of every three buildings over an area of  $11 \text{ km}^2$  were ablaze just within 20 minutes after the first wave of bombers had passed. A 3 km high,  $2 \frac{1}{2} \text{ km}$  base diameter column of burning gases was noted. At a distance of  $2 \frac{1}{2} \text{ km}$  from the fire zone, winds as high as 17 to 53 km/hr were induced to uproot trees 0.9 m in trunk diameter. Due to a  $40 \text{ km}^2$  fire in Tokyo in 1945, induced winds were noted to be 45-88 km/hr at a distance of  $1 \frac{1}{2} \text{ km}$  from the periphery of the fire; upward flow was so strong that aircraft flying at an altitude of 1 800 meters over the fire zone were overturned.

Faure reports an important experimental fire on a 325-hectare (803-acre) plot of 1 m high bushes and thornbroom. The flames were observed to be as high as 10 to 12 m. The 5 to 8 m/s prevailing wind did not seem to have much of an effect on the smoke column upto about 500-600 m altitude. The fuel load was estimated to be near  $1.7 \text{ kg/m}^2$  ( $1/3 \text{ lbm/ft}^2$ ) and the fuel element combustion time was about 35 minutes. Assuming that the fuel has a heat of combustion of about 16,000 kJ/kg, the heat release rate is estimated to be about  $3.7 \times 10^5$  megawatts. Also assuming stoichiometric air/fuel ratio to be  $3.3 \text{ m}^3/\text{kg}$  ( $53 \text{ ft}^3/\text{lbm}$ ), the air consumed in combustion is expected to be  $1.6 \times 10^8 \text{ m}^3$  total at a rate of  $8,000 \text{ m}^3/\text{s}$ . The average required entrainment

velocity over a rim of 10 m high around the periphery of equivalent diameter of 2,000 m thus is about 1.25 m/s. The observed air speed 100 m from the fire ranged between 10 to 15 m/s which at the fire rim is expected to reflect in an actual entrainment speed of about 11-17 m/s. Thus, the air actually entrained is over 10 times larger than that required for combustion; this is in total agreement with the general knowledge that nearly all fires induce a 1,000% excess air. With this indicated excess air, the fire gases entering the base of the plume can be estimated to be at about 400 K. The 'smoke column' was noted in the test to have reached an altitude of about 2300 m where it became horizontal.

Faure also attempts to draw the scale modeling rules for the flow and combustion phenomena associated with very large fires and the plumes over them. But little is done to demonstrate the utility of the developed rules. A similar comment is valid also for an elegant note prepared by Byram [51].

An investigation of the turbulent natural convection plume above a circular ring fire has been reported by Lee and Ling [52]. As a fire grows gradually, say in a circular pattern, the interior of this circular area will be 'burnt out', sooner or later. A result is a fire which is a ring of finite width spreading outwards. A dimensional analysis is presented to arrive at the following velocity and temperature scaling in terms of our earlier-defined characteristics.

$$W, U = \frac{w, u}{\left( \frac{\beta^2}{(\beta^2 + 1)} \frac{Q}{2r_0} \right)^{1/3}} \quad (9.28)$$

$$\theta = \frac{g(T - T_\infty)/T_\infty}{\frac{1}{r_0} \left( \frac{\beta^2}{(\beta^2 + 1)} \frac{Q}{2r_0} \right)^{2/3}} \quad (9.29)$$

where  $w$  is the upward velocity,  $u$  is the inward, radial, (entrainment) velocity,  $r_0$  is the mean radius of the ring-fire-base,  $\beta^2 \sim 96/71$  is the Rouse constant and  $Q$  is the buoyancy input  $[r_0^2 u_{\max} g(\rho_\infty - \rho)_{\max}/\rho_\infty](m^4/s^3)$ . These scaling relations are essentially same as those of Priestley and Ball and of Morton, Taylor and Turner. Measurements made in the plume of a propane fire over a 29-inch diameter burner have been correlated on the basis of the developed dimensional analysis. Among a number of interesting conclusions,

the following two are of our immediate consequence. First, as one plots the entrainment velocity  $U$  as a function of nondimensional radius ( $R \equiv r/r_0$ ), for various axial locations  $Z(\equiv z/r_0)$  and various characteristic velocities  $\omega(\equiv [\beta^2 Q / (2r_0(\beta^2 + 1))]^{1/3})$ , one finds that it: (a) is virtually independent of  $\omega$ ; (b) increases with increasing  $Z$  ( $U_{\max} \approx 2$  at  $Z \approx 0.5$  and  $\approx 2.5$  at  $Z \approx 4$ ); and (c) increases from zero at  $R = 0$  to a maximum near about  $R = 0.5$  and then decays as  $R$  increases; at the rim,  $R = 1$ ,  $U$  is about 50% of its maximum value. In physical terms, the maximum entrainment velocity noted in these 29-inch diameter fires is about 6.5 ft/s. That the maximum entrainment velocity occurs within the fire with the attendant pressure-field consequences and that the velocity and temperature fields scale well within the context of  $\omega$  are perhaps the two most important contributions of this work of Lee and Ling.

W. J. Parker, Corlett and B. T. Lee [53] conducted scale model tests of a mass fire (Flambeau, Countryman [54]) using a 0.61 m x 0.61 m (2 ft x 2 ft) electrical heat source of strength 12.7 kW/m<sup>2</sup>. The Flambeau fire was 335.3 m x 320 m (1100 ft x 1050 ft) in extent. The length ratio between the Flambeau and the model thus is 537. At 18 minutes after ignition, the Flambeau test indicated a heat release rate of about 200 kW/m<sup>2</sup> (1060 Btu/ft<sup>2</sup> min). At an elevation of 15.24 m (50 ft) at the center of one edge of the Flambeau plot, induced velocity was measured to be fluctuating between about 3 and 5 m/s (10 and 16 ft/s), steady after about 18 minutes past ignition. The Parker, Corlett, Lee model yields a velocity of 0.195 m/s at a height of 0.028 m (which is homologous to 50 ft). With the scaling argument that  $u \propto \sqrt{L}$ , these modelers convert this measured model velocity to the prototype Flambeau velocity of  $u_{\text{Flambeau}} = u_{\text{model}} \times \sqrt{(L_{\text{Flambeau}}/L_{\text{model}})} = 0.195\sqrt{537} = 4.52$  m/s, which is within the range of the Flambeau fluctuation measurement. The scaling argument that  $u \propto \sqrt{L}$ , however, is in some variance with the general knowledge of plume scaling discussed earlier in this chapter. Some considerations of this work related to the specific details of the combustion zone will be discussed later in section (f) of this report.

9.4 Firebrand Transport: The convective currents produced by the fire will bring about an enhanced air supply to the burning fuel; the feed-back heat flux is thereby enhanced as well. Intense heating is expected to produce mechanical disruption of the burning fuel elements to generate firebrands -- namely fragments of fuel which continue burning in flight. The blast-produced debris fuel piles are expected to be copious sources of firebrands. Given the initial size distribution of the firebrands along with upward convective plume velocity and the prevailing wind, the problem at hand is to map out the firebrand trajectories. Continued pyrolysis (and burning) of a firebrand in the course of its flight is itself expected to significantly influence the trajectory. The topics of concern, in order, are the production, consumption (life-time) and transport of the brands. There exists little quantitative or qualitative information on the issue of production. One can note, however, that both the number and size of brands produced may be expected to depend upon the rate of heating of the fuel (and, hence, on the stage of growth and intensity of burning of the fire) and upon the nature of the fuel itself. There is urgent need to develop these dependencies which are perhaps amenable only to empirical studies.

Combustive consumption of wood particles in the forced convection conditions of flight is described by Tarifa, del Notario and Moreno [55]. Both the density of the solid ( $\rho_w$ ) and the size of the particle ( $r$ ) are noted to decrease with time ( $t$ ) according to

$$\frac{\rho_w}{\rho_{w0}} = \frac{1}{(1 + \eta t^2)} \quad (9.30)$$

$$\frac{r}{r_0}^2 = 1 - \frac{\beta + w\delta}{r_0^2} t \quad (9.31)$$

where the subscript 0 represents the initial conditions.  $w$  is the relative wind speed about the firebrand. The constants  $\eta$ ,  $\beta$  and  $\delta$  (with units respectively of  $1/\text{sec}^2$ ,  $\text{m}^2/\text{s}$  and  $\text{m}$ ) are empirically determined combustion properties of the wood with a given moisture content. Tarifa notes that the relative wind speed  $w$  is not significantly different from the particle's instantaneous terminal velocity  $w_f$  which depends on the instantaneous size as



well as mass of the particle as

$$w_f = w_{f0} \left( \frac{\rho_w}{\rho_{w0}} \frac{r}{r_0} \right)^{1/2}. \quad (9.32)$$

Thereby, Tarifa obtains the following implicit relation for the particle size variation with time.

$$\left( \frac{r}{r_0} \right) = \left\{ 1 - \frac{gt}{r_0^2} - \frac{\delta w_{f0} t}{r_0^2} \frac{1}{(1 + nt^2)^{1/2}} \left( \frac{r}{r_0} \right)^{1/2} \right\}^{1/2} \quad (9.33)$$

$w_{f0}$  in these relations is the initial terminal velocity of the brand prior to any significant reduction in size and mass is experienced.

Describing then the equation of motion of the flying brand by balancing its inertia with drag and gravity forces, Tarifa computes the flight trajectory numerically under conditions of constant wind. The fall velocity can be expressed as

$$w_f(t) = \left\{ \frac{m(t) g}{\frac{1}{2} C_D(t) \rho_\infty A(t)} \right\}^{1/2} \quad (9.34)$$

where  $m$  is instantaneous mass of the brand,  $g$  is gravity,  $C_D$  is drag coefficient,  $\rho_\infty$  is ambient air density and  $A$  is the brand frontal area. The main difficulty, even if the brand geometry is simplified to spheres and short cylinders, was that both the drag coefficient and the mass of the brand were complicated functions of time due to variation in size and density. Among the computed quantities is the time ( $t_g$ ) required for the brand to reach the ground. Comparing this time with the experimentally determined burn-out time ( $t_b$ ) of the brand, one can reach certain critical conclusions. If  $t_b > t_g$ , then firebrand reaches the ground while still burning, thus capable of initiating a fire upstream. If  $t_b < t_g$ , the brand is burnt-out in the flight. The maximum horizontal range within which spotting fires can be initiated by the flying brands is given by the condition  $t_b = t_g$ .

Notwithstanding the need to employ empiricism in describing the combustion of the firebrands, it is fitting to note that the concept underlying the firebrand flight methodology of Ref. [55] is indeed meritorious. Tarifa himself promptly recognizes this and presents a

dimensional analysis in Ref. [56]. Two cases are considered: first, the firebrand undergoes combustion in a wind of constant speed; and second, the firebrand burns as it flies at its final fall velocity.

Denote the ratio of final fall velocity of the brand to the initial fall velocity  $w_f/w_{f0}$  by the symbol  $\xi$ . For spherical and cylindrical brands, the experimental data indicate that this ratio depends only on a nondimensional quantity  $U_1$  defined as

$$U_1 \equiv \chi \text{Re}^{-0.4} \xi^{1.3} \lambda_1^{-0.4} \quad (9.35)$$

where  $\chi \equiv wt/d_0$  (with wind speed  $w$ , time  $t$  and the particle diameter  $d_0$ );  $\text{Re} \equiv wd_0/\nu_\infty$  is the Reynolds number ( $\nu_\infty$  being the kinematic viscosity of ambient air);  $\xi \equiv \rho_\infty/\rho_{w0}$  is the ratio of the ambient air density to the initial density of the brand-wood; and  $\lambda_1$  is a geometric ratio of the brand ( $\lambda_1 = \text{length/diameter ratio for cylinders and } \lambda_1 = 1 \text{ for spheres}$ ). The burn out time  $x_b$  is found from the experimental correlations to be given by  $U_1 = U_{1b} = 2.6$ .

In the second case, the firebrands are considered to be burning within an air current whose velocity is constant and equal to the brand's final fall velocity. In this case  $\chi$  and  $\text{Re}$  are defined on the basis of the initial fall velocity  $w_{f0}$ . Then the expression for  $U$  remains same as in the first case for cylindrical and spherical particles. For square plate particles, however,  $U = U_1 \times 0.6\lambda_2$  where  $\lambda_2$  represents the additional required length ratio in the particle description.

In order to further employ Tarifa's methodology, considerable further work on the behavior of firebrand burning is required. Various particle shapes and ranges of initial size have to be considered on different materials. Two recent works in these directions are: Lee and Hellman [57] and Muraszew, Fedele and Kuby [58].

9.5 Fire and Wind/Fire Storms: When the fire is large enough in size and in intensity, the convective flows prompted by it may be strong enough to noticeably interfere with the atmosphere itself. Considerable research in this area has been reported in the literature by Morton [59], Long [60], Muraszew, Fedele and Kuby [58], Small and Brode [61] and Carrier, Fendell and Feldman [62].

Morton's paper is essentially a qualitative description of the flows induced by large fires, conflagratory fire spread as influenced by the ambient winds, and the origin of blow-up -(or back-) fires which generate vorticity to cause fire-tornadoes. Two points made in this paper are noteworthy. First, whereas the entrainment occurs at all heights with a velocity about an order of magnitude smaller than the mean upward velocity in the plume, the radial pressure field near the ground tends to amplify the local entrainment. This amplified, near-ground, entrainment reflects in the induced winds. Furthermore, it is expected to intensify the combustion rate of the loosely packed fuel bed not only by the increased air supply and its mixing with the fuel vapor but also by augmenting the heat flux from the flame to the fuel elements.

The second point concerns with the effect of (back-) fires which are started by such agents as firebrands. Known also as blow-up fires, they tend to develop strong rotational flow with a concentrated vortex cone to yield the phenomena of fire-whirls and fire-tornadoes. These phenomena themselves serve to transport the firebrands to greater altitudes and greater horizontal reaches. Thus, the problem obviously is of strong nonlinearity within which discernment of cause and effect is not at all a clear-cut exercise. The strong buoyant flow in the plume and the associated entrainment are also known to amplify the vorticity which is dilutely present in the atmosphere.

Long [60] presents an analysis of the fire-whirl. The buoyant fire plume entrains and amplifies the atmospheric vorticity. While the vorticity due to earth's rotation is of the order of  $10^{-4}$ /sec, a hundred times larger vorticity is required to produce a fire-whirl. Sources of such a larger ambient vorticity may be local meteorological eddies or cyclones with length scales less than a mile or so. Gravitational instability, light wind and low humidity of air are noted by Long to be conditions conducive for a firestorm.

Long deduces an interesting scaling scheme for firestorms (ignoring radiation, treating the fire as a buoyancy source by simply specifying a temperature  $T_f$  in the fire of diameter  $d$ , higher than in the ambient air  $T_\infty$ , neglecting the Coriolis force due to earth's rotation (i.e., the Rossby number is much greater than unity), considering that the curvature of the earth is inconsequential and that all molecular transport processes are unimportant). The nondimensional parameters to be preserved between the model and prototype are:

$$k' \equiv k/d \quad (9.36)$$

$$\epsilon \equiv \frac{\alpha \Omega^{2/3} d^{4/3}}{g^{1/3} (\Delta \bar{\rho} / \bar{\rho}_0)^{4/3}} \quad (9.37)$$

$$s \equiv \Delta \bar{\rho} / \bar{\rho}_0 \quad (9.38)$$

$$F \equiv \left[ \frac{\Omega^2 d}{g (\Delta \bar{\rho} / \bar{\rho}_0)} \right]^{2/3} \quad (9.39)$$

$$m^2 \equiv \left[ \frac{g^2 \Omega^2 d^4}{(\bar{P}_0 / \bar{\rho}_0)^3 (\Delta \bar{\rho} / \bar{\rho}_0)} \right]^{1/3} \quad (9.40)$$

$$\sigma \equiv \text{adiabatic exponent, } C_p/C_v \approx 1.4 \quad (9.41)$$

The parameters  $s$ ,  $m$  and  $\sigma$  are thermodynamic in nature.  $\bar{\rho}$  is potential density, a conserved quantity, of the fire gases;  $\bar{\rho}_0$  is potential density of the ambient air;  $\Delta \bar{\rho} \equiv \bar{\rho}_0 - \bar{\rho}$ . If the model and prototype fires are of same temperature,  $s$  is automatically preserved. So also is  $\sigma$ . The parameter  $m$  is indicative of the compressibility effects. ( $g$  is gravity,  $\Omega$  is angular velocity of solidus rotation of the ambient fluid;  $d$  is fire diameter;  $\bar{P}_0$  is potential pressure of the atmosphere.) Even for a fire as large as  $d \approx 1500$  m, the parameter  $m^2$  is seldom larger than about  $10^{-3}$  for typical values of  $\Omega$ ,  $\bar{P}_0/\bar{\rho}_0$  and  $\Delta \bar{\rho}/\bar{\rho}_0$ . It could thus be safely disconcerting.

Of the remaining three parameters,  $\epsilon$  is a measure of the gradient of potential density with altitude. In its definition,  $\alpha$  is a constant related to the stability of the atmosphere. For a near-neutrally stable atmosphere which is recognized to be conducive for a firestorm,  $\alpha \approx 0$  so that  $\epsilon \approx 0$ . Thus, Long rules out the importance of  $\epsilon$  in the scaling endeavors so long as care is taken to keep it near zero. One then is left with only two parameters of concern.  $k'$  is the ratio of surface roughness length  $k$  (due to buildings in a city or trees in a forest) to the fire diameter  $d$ . Keeping  $k'$  invariant, therefore, implies satisfying geometric similarity.

Since  $g$  and  $s$  are same in both the model and the prototype, one has to adjust the external fluid rotation  $\Omega$  with fire size  $d$  so as to maintain the

important parameter  $F$  invariant. Thus, to simulate a  $d = 1500$  m fire (in an atmosphere containing a  $\Omega = 10^{-3}/s$  rotation) by a model of  $d = 15$  m,  $\Omega$  has to be adjusted to  $10^{-2}/s$ . This can be achieved by mechanical means.

While  $k'$  and  $F$  thus are the primary scale parameters to simulate a firestorm, Long's analysis indicates that the pressure, density, radial location, velocities and time would scale according to the following nondimensionalization with  $L \equiv [\Omega^2 d^4 / g(\Delta \bar{\rho} / \bar{\rho}_0)]^{1/3}$ .

$$P^* \equiv P' / gL \Delta \bar{\rho} ; \quad \rho^* \equiv \bar{\rho}' / \Delta \bar{\rho} ; \quad r^* \equiv r / L ; \quad (9.42)$$

$$v^* \equiv v / [gL \Delta \bar{\rho} / \bar{\rho}_0]^{1/2} \quad \text{and} \quad t^* \equiv (t/L)[gL \Delta \bar{\rho} / \bar{\rho}_0]^{1/2} . \quad (9.43)$$

If there were no rotation whatsoever is present,  $\Omega$  will be zero; the characteristic length becomes  $d$  in these definitions;  $F$  will be zero.  $m^2$  and  $\epsilon$  respectively become  $gd/(\bar{P}_0/\bar{\rho}_0)$  and  $\alpha d/(\Delta \bar{\rho}/\bar{\rho})$ ;  $m^2$  will still be negligible;  $\epsilon$  will remain near zero for both the model and prototype; and the modeling endeavors reduce to keeping thermodynamics invariant and preserving geometric similarity. Suffice it to note in conclusion that Long's paper holds a wealth of ideas pertaining to scaling mass fires, especially firestorms; it should be a standard reference in all fire-modeling efforts.

9.6 The Combustion Zone Specifics: Once the heat output of a fire over a given area at altitude zero is given, it is clear from the preceeding discussions that the character of buoyant plume flow is scaleable. To determine the pyrolysis and burning rate of the fuel deris is thus a crucial aspect to be discussed below.

As a condensed-phase fuel element is heated, convectively due to contact with the hot flame gases or radiatively due to remote flames and glowing charcoal, it first heats-up and then undergoes pyrolysis (or simple physical vaporization) to yield combustible pyrolyzate gases and vapors. Upon mixing with the oxygen of the ambient air, these pyrolyzates result in fresh flames which may themselves furnish further fuel-heating energy. The problem of combustion intensity thus entails a study of heat and mass transfer across the fuel element boundary. While conductive heating and subsurface pyrolysis processes predominate within the fuel element, convection and oxidation reactions dominate in the gas-phase (and at the interface). Thermal radiative heat exchange may become relevant both within and outside the porous fuel element.

When an isolated fuel element is subjected to radiative and convective heating, the steady state pyrolyzate efflux rate  $\dot{m}''$  ( $\text{kg}/\text{m}^2\text{s}$ ) can be written, by a linear approximation, as

$$\dot{m}'' = [\dot{q}''_{\text{rad}} + h(T_{\infty} - T_w)]/L_{\text{sg}} \quad (9.44)$$

where  $\dot{q}''_{\text{rad}}$  is net radiant flux received by the surface,  $h$  is heat transfer coefficient,  $T_{\infty}$  is the flame gas temperature,  $T_w$  is the surface temperature of the pyrolyzing fuel element and  $L_{\text{sg}}$  is the latent heat of pyrolysis ( $\text{J}/\text{kg}$  pyrolyzate). With  $C_{\text{pg}}$ ,  $K_g$  and  $\ell$  respectively representing the gas-phase specific heat, conductivity and the specimen characteristic dimension, the above equation can be written nondimensionally as follows:

$$\left[ \frac{\dot{m}'' C_{\text{pg}} \ell}{K_g} \right] = \left[ \frac{\dot{q}''_{\text{rad}} C_{\text{pg}} \ell}{K_g L_{\text{sg}}} \right] + \left[ \frac{h \ell}{K_g} \right] \left[ \frac{C_{\text{pg}} (T_{\infty} - T_w)}{L_{\text{sg}}} \right] \quad (9.45)$$

The left-hand-term is nondimensional pyrolyzate efflux rate. The first term on RHS accounts for the radiant heating while the second term accounts for convective heating. The quantity  $(h\ell/K_g)$  is known as Nusselt number, a function of fluid mechanics of flow (i.e., of Reynolds or Grashof number and Prandtl number). The enthalpy ratio  $[C_{\text{pg}}(T_{\infty} - T_w)/L_{\text{sg}}]$  is a descriptor of the thermodynamics of combustion (numerator) and pyrolysis (denominator); this ratio is known as the B-number.

The role of radiative heating may be viewed in different view-points. First, rewriting the preceeding relation in the following form,

$$\left[ \frac{\dot{m}'' C_{\text{pg}} \ell}{K_g} \right] = \left[ \frac{h \ell}{K_g} \right] \left[ \frac{C_{\text{pg}}}{L_{\text{sg}}} \left( T_{\infty} + \frac{\dot{q}''_{\text{rad}}}{h} - T_w \right) \right] \quad (9.46)$$

the effect of radiation may be taken as an apparent increase in the flame temperature to augment the convective heat transfer rate. Alternatively,

$$\left[ \frac{\dot{m}'' C_{\text{pg}} \ell}{K_g} \right] = \left[ \left( h + \frac{\dot{q}''_{\text{rad}}}{(T_{\infty} - T_w)} \right) \frac{\ell}{K_g} \right] \left[ \frac{C_{\text{pg}} (T_{\infty} - T_w)}{L_{\text{sg}}} \right] \quad (9.47)$$

whereby, radiation may be viewed to have increased the convective heat transfer coefficient. Finally, if  $\dot{q}''_{\text{rad}} / [h(T_{\infty} - T_w)]$  is small compared to unity,

$$\left[ \frac{\dot{m}'' C_{pg} \ell}{K_g} \right] \approx \left[ \frac{h \ell}{K_g} \right] \left[ \frac{C_{pg}(T_{\infty} - T_w)}{L_{sg}(1 - [\dot{q}''_{\text{rad}}/h(T_{\infty} - T_w)])} \right] \quad (9.48)$$

implying that the presence of radiant heating tends to manifest in a reduction of the enthalpy of pyrolysis.

This simple linear analysis is thus quite instructional as to the manner in which thermal radiation intrudes to augment the convective pyrolysis rate of a fuel element. Exact analyses solving the differential equations governing the heat and mass transfer process are available to remove the present simplification of linearity. But the fundamental nondimensional parameters remain unaltered.

It then remains, in scaling the heating process of a fuel element, a trivial task to estimate the radiant flux  $\dot{q}''_{\text{rad}}$  and to obtain the Nusselt number ( $h \ell / K_g$ ) as a function of Reynolds (or Grashof) and Prandtl numbers. Existing heat transfer literature enables us to perform this task quite well. The main difficulty, however, lies in the fact that the fires of present concern involve fuel beds which are nonuniform and fuel elements in these beds are random in size, shape and orientation. This difficulty may be overcome, perhaps, only by a stochastic description of the structure of the fuel bed. Such descriptions, however, are presently unavailable. Notwithstanding this unavailability, it is perhaps worth noticing how Rothermel coped with this fuel description problem.

In order to study the forced convective combustion of fuel element debris piles, Strasser and Grumer [63] reported an interesting experiment. 4 kg of 2x2x4 cm wood pieces were piled randomly in a wire basket, ignited with a methanol accelerant and combustion rate was monitored. The rate quickly attains a maximum ( $\approx 4.8$  g/s) and then gradually decays. The air flow induced into the fuel-bed was modeled by a well-known relation of the pressure drop through packed beds with turbulent flow [64]. In the balance of the pressure drop with buoyancy and inertia, it has been found that the inertia effect is minimal. The velocity of air induced through the peripheral area of the

vertical circular cylinder of a debris pile (height =  $H_{bed}$ , diameter =  $d_{bed}$ ) was found to depend upon the ambient air temperature  $T_{\infty}$ , the burned gas temperature  $T_b$  exiting out of the pile at the top, the diameter of the fuel particles  $d_{particle}$  composing the bed whose void fraction is  $\delta$ , the friction factor  $f$  which is a weak function of the Reynolds number, and a particle shape factor  $\lambda$ .

$$\frac{u_{induced}}{[g H_{bed} (T_b - T_{\infty}) / T_{\infty}]^{1/2}} \approx (T_{\infty} / T_b) \left\{ \frac{\delta^3 d_{particle} / d_{bed}}{f \lambda^{1.1} (1 - \delta)} \right\}^{1/2} \quad (9.49)$$

The velocity thus calculated was not only in excellent agreement with the measured but also equal to the stoichiometric requirement for the wood-burning. Recall, from our estimates in the context of Faure's field experiment, that wood-like fuels require about  $3.3 \text{ m}^3$  ( $\approx 4 \text{ kg}$ ) of ambient air to stoichiometrically burn 1 kg of the fuel. Thus, the burning rate  $\dot{m}_F$  (kg fuel/sec) of the debris basket appears to obey the relation

$$\frac{3.3 \dot{m}_F / \rho_{\infty} \pi d_{bed} H_{bed}}{[g H_{bed} (T_b - T_{\infty}) / T_{\infty}]^{1/2}} \approx (T_{\infty} / T_b) \left\{ \frac{\delta^3 d_{particle} / d_{bed}}{f \lambda^{1.1} (1 - \delta)} \right\}^{1/2} \quad (9.50)$$

While, thus, the air induced into the fuel bed itself satisfies the stoichiometry, the flames are expected to project above the fuel bed to a height of the order of fuel bed diameter for small but turbulent fires and of the fuel bed height for large fires. It is these flames which induce great quantities of excess air to dilute the flame gases.

The maximum burning rate  $\dot{m}_{max}$  measured by Strasser and Grumer is such that the burn time of a fuel element of initial mass of  $m_0$  is in the range  $1200 < m_0 / \dot{m}_{max} < 2800 \text{ sec}$  for Douglas fir sticks in the range  $2 \text{ cm} < d_{particle} < 9 \text{ cm}$ . When a fan blows air into the flame column, no discernible change in burning rate was noticed. However, if it blows air into the fuel bed, the burning rate is enhanced somewhat in proportion to  $\sqrt{(u_{wind} / d_{particle})}$ .

Attempts to progressively increase the size of laboratory fires have always yielded the result of disintegration of the flame into multiple flamelets. (See also Corlett [65], Blackshear [66] and Wood, Blackshear and



Eckert [67].) When the fire base diameter is less than 10 m, the visible flame height is approximately equal to the base diameter. At larger base diameters, however, the flame height is much smaller than the base diameter and the flame appeared to be composed of multiple, individual flamelets which move around the base in an unsteady way almost as though the heat feed-back and vaporization processes are nonuniform.

Attempts to model the interaction of multiple adjacent flames (Putnam and Speich [68], Welker and Sliepcevich [31]) are less than completely successful. Whereas flames separated widely tended to mutually augment the burning rate (presumably due to enhanced heat feed-back), flames separated but only narrowly tended to experience lowered burning rate (presumably due to competition for oxygen). Reference [63] presents some data relevant to this behavior. When two 26 cm high fuel beds composed of 4 cm cubes of Douglas fir fuel elements were burned side-by-side, the maximum burning rate increased from 3.3 g/s when separation is large to a maximum of about 5 g/s at a separation of about 0.1 m and then decreased to about 3.7 g/s when separation is zero. It was concluded that radiative heat transfer between proximate fires augment the burning rate less than convective heat transfer does. Strasser and Grumer [63] arrive at the opinion that a metastable atmosphere is perhaps a prerequisite for multiple fires to merge to form a firestorm and that in such a situation, combustion occurs within (and/or very close to) the fuel bed.

Parker, Corlett and B. T. Lee [53] also come to a similar conclusion based on the following two points. First, in large fires, molecular transport processes are almost insignificant relative to turbulent mixing. The Grashof number is thus realized to be so large as to be irrelevant in mass fire scaling. Second, the flames and product gases in large fires are optically thick in the wavelength range of concern; the Rosseland diffusivity of such a medium is infinitesimally small compared to the turbulent eddy diffusivity for heat transport. The net consequence of this is that radiative transport within a mass fire is expected to be dominant only in a thin zone near the fuel bed. It must thus be permissible to model mass fires by employing an electrical (area) heat source near the ground surface in the laboratory.

Having thus simplified, the mass fire problem is reduced to a thermally driven fluid mechanics problem whose working fluid is normal air. The combustive energy input then can be expressed as a merely nondimensional heat

feed-back flux

$$\tilde{Q} \equiv \frac{\dot{q}''}{(g \lambda)^{1/2}} \frac{1}{\rho_{\infty} C_{p\infty} T_{\infty}} \quad (9.51)$$

where  $(g \lambda)^{1/2}$  is the characteristic velocity,  $\lambda$  is the fuel bed dimension and  $\dot{q}''$  is the heat flux ( $W/m^2$ ). The heat release rate thus being proportional to  $\sqrt{\lambda}$ , a 600 m ( $\approx 2000$  ft) fire releasing energy at a rate of about  $3 \text{ MW/m}^2$  ( $\approx 10^6$  Btu/ft<sup>2</sup>/hr) is expected to be scaleable by a 0.6 m ( $\approx 2$  ft) laboratory fire with a heat flux of  $95 \text{ kW/m}^2$  ( $\approx 30,000$  Btu/ft<sup>2</sup>/hr). This small a laboratory fire, albeit turbulent, is indeed a weak one exhibiting an irregular flame hovering erratically about the fuel surface 'with much openness' [53]. Corlett, too, concludes that without the effects of vertical atmospheric vorticity, a firestorm will most probably not arise.

While these considerations attempt to capture the essential heat transfer mechanisms between the flames (and hot gases) and the surface of a fuel element, it is fitting to briefly examine the scaling principles involved in the manner in which the solid fuel element utilizes the energy received. As the solid heats up due to transient conduction, it eventually undergoes thermal degradation at all depths. The pyrolyzates thus produced transpire out of the char into the flaming surroundings.

Tarifa [55] notes from wind-tunnel experiments that the density of wood decreases with time according to an inverse quadratic function of time:  $\rho_w/\rho_{w0} = 1/[1 + n t^2]$  where  $n$  is an empirical constant characteristic of the nature of wood. He also finds that the diameter of the fire brand decreases according to a square-law:  $(d/d_0)^2 = 1 - [4(\beta + w\delta)/d_0^2]t$  which is analogous to the well-known square-law associated with liquid fuel droplet combustion. (Recall that  $\beta$  and  $\delta$  are empirical constants and  $w$  is wind speed.)

An analysis of charring conduction presented by the present author [69] sheds further light on the nature of combustion of wood-like fuel elements. The main result of this analysis is the following time-dependency of the mass  $m$  of the charring element.

$$\frac{m(t)}{m_0} = \frac{\rho_c}{\rho_0} + \left( \frac{\rho_0 - \rho_c}{\rho_0} \right) \left( 1 - \frac{t}{t^*} \right)^{(j+1)/2} \quad (9.52)$$

where  $m_0$  is initial mass,  $\rho_c$  and  $\rho_0$  are final char and initial wood densities,  $t$  is time and the index  $j$  is 0 for an infinite slab, 1 for a long cylinder and 2 for a sphere. The characteristic burn-out time  $t^*$  is given by

$$\left( \frac{\alpha_0 t^*}{\ell_0^2} \right) = \left( \frac{(3+j)L_{sg}(\rho_0 - \rho_c)/2 + \rho_0 C_{p0}(T_p' - T_0)}{(1+j)\dot{q}'' \ell_0/\alpha_0} \right) + \frac{1}{2(3+j)} \quad (9.53)$$

where  $\ell_0$  is the initial half-thickness of the particle,  $L_{sg}$  is enthalpy of pyrolysis (kJ/kg pyrolyzate),  $C_{p0}$ ,  $\alpha_0$  are respectively the specific heat and thermal diffusivity of wood,  $T_p'$  is a temperature characteristic of the pyrolysis process,  $T_0$  is wood's initial temperature, and  $\dot{q}''$  is the heat flux received by the surface from the ambient gas-phase. Two major points are evident from these results: (a) The mass loss rate depends on the time function  $(1 - t/t^*)$  raised to a power of  $-1/2$  for a slab, 0 for a cylinder and  $+1/2$  for a sphere. For cylindrical fuel elements, thus, the rate is apparently independent of time. (b) The terms on the RHS of the  $(\alpha_0 t^*/\ell_0^2)$  equation respectively represent the thermochemistry of pyrolysis and thermal diffusion. When thin fuel elements are considered, the thermochemical term dominates to make visible the influence of pyrolysis endothermicity  $L_{sg}$ , pyrolysis kinetics  $T_p'$  and the heating rate  $\dot{q}''$ . When the fuel elements are thick, however, the second term dominates indicating that thermal diffusion overwhelms all the thermochemical and thermokinetic details as well the exposure flux specification itself. With  $L_{sg} \approx 300$  kJ/kg,  $\rho_0 \approx 600$  kg/m<sup>3</sup>,  $\rho_c \approx 150$  kg/m<sup>3</sup> and  $\alpha_0 \approx 10^{-7}$  m<sup>2</sup>/s, the above result becomes

$$t^* \approx \left( \frac{3+j}{1+j} \right) \times 6.75 \times 10^7 \times \frac{\ell_0}{\dot{q}''} + \left( \frac{1}{3+j} \right) \times 5 \times 10^6 \times \ell_0^2 \quad (9.54)$$

where  $\ell_0$  is in meters,  $\dot{q}''$  is in Watts/m<sup>2</sup> and  $t^*$  is in seconds. If  $\dot{q}''$  is 20,000 W/m<sup>2</sup>, for cylindrical dowels,  $t^* \approx 6.75 \times 10^3 \ell_0 + 1.25 \times 10^6 \ell_0^2$  so that fuel elements thicker than about a centimeter, or so, will behave as though they are thermally thick and the pyrolytic time is determined more by the diffusion effects than by the chemical, kinetic, and exposure effects.

## SECTION 10

### CONCLUDING REMARKS

Based on the foregoing discussions, it is eminently clear that much can be done to improve our understanding of the behavior of a large real fire by employing the technique of scale modeling. At the heart of the design of a scale model lies the need to recognize the physicochemical mechanisms involved in the character of the modeled fire. This recognition can evolve from either a sophisticated theoretical formulation of the problem (but with no need to solve it) or a mere dimensional analysis (in which a dimensional assessment is made of all the involved dependent and independent variables). The main objective of a scale model design exercise is to identify combinations of variables of the problem so that a relationship among these combinations may be easier determined experimentally without destroying the generality of the relationship. In other words, the behavior patterns of the phenomenon under study will be quantitatively expressible as relations between the variable combinations such that the proportionality constants and indices of powers are independent of the system and even of the materials employed. The combinations of variables are nondimensional; they serve to relate the scale model homologously with the prototype and, as such, are known as scaling prescriptions.

Becoming thus impressed with the tremendous proven power of scale modeling in various engineering disciplines, attempts to apply this art in studies of fire behavior quickly lead one to conclude that complete modeling of such a complex system is impossible, for the number of prescription rules far exceed the experimenter's degrees of freedom. The reader is encouraged to refer to Professor Spalding's superb exposé [8] to truly appreciate the difficulties associated with complete modeling of combustion systems.

We are thus convinced that we should become content with modeling of the mass fire in parts. The contents of the present report indicate that the mechanistic description of various aspects of a mass fire is not only possible but also mostly available in the existing literature. These aspects range from the inception of the fire to the fully developed plumes. The state-of-the-art of current understanding of these aspects is so advanced that the scaling rules can be relatively easily deduced.

The question facing immediately is: Which aspect or aspects of the mass

fire is it that we wish to scale model? The answer obviously depends upon the "interests of the experimenter and the accuracy and urgency of the required prediction" [8]. Once this choice for partial modeling is made, scaling prescriptions can be deduced to specifically highlight the effects sought; scale model experiments can be designed to satisfy these prescriptions; experiments can be conducted; and their results can be generalized.

Evident from the work reported here are some areas in which the existing mechanistic understanding leaves further progress desired. Some of these areas are: the mechanisms of fire growth within enclosures to flashover; the role played by thermal radiation heat transfer in a number of contexts of fire growth, conflagratory speed, intensity of burning and others; the mechanism of production of firebrands in large fires; the phenomenon of firebrand burning in flight; and the specific details of combustion of fuel elements in the intense environment of debris piles.

## SECTION 11

### LIST OF REFERENCES

1. S.B. Martin, "Diffusion-Controlled Ignition of Cellulosic Materials by Intense Radiant Energy," pp. 877-896, Tenth Symp. (International) on Combustion, The Combustion Institute, Pittsburgh, PA (1965).
2. A.M. Kanury, "Ignition of Cellulosic solids--A Review," Fire Research Abstracts and Reviews, 14, pp. 24-52, (1972).
3. P.D. Gandhi, "Spontaneous Ignition of Organic Solids by Radiant Heating in Air," Ph.D. Dissertation, University of Notre Dame, Notre Dame, IN (1984).
4. A.M. Kanury, "Scaling Correlations of Flashover Experiments," Paper to appear in ASTM STP entitled Application of Fire Science to Fire Engineering, T.Z. Harmathy, Editor, American Society for Testing and Materials, Philadelphia, PA (1985).
5. A.M. Kanury, "Response Mechanism: Blast/Fire Interactions," Final Report, Contract No. EMW-C-0366 WU No. 2564 H, Federal Emergency Management Agency, Office of Mitigation and Research, Washington, DC (1983).
6. G. Murphy, Similitude in Engineering, The Ronald Press Company, New York, NY (1950).
7. L.A. Segel, "Simplification and Scaling," SIAM Review, 14(4), pp. 547-571, (1972).
8. D.B. Spalding, "The Art of Partial Modeling," pp. 833-843, Ninth Symp. (International) on Combustion, The Combustion Institute, Pittsburgh, PA (1963).
9. F.A. Williams, "Scaling Mass Fires," pp. 1-23, Fire Research Abstracts and Reviews, 11(1), (1969).
10. S. Glasstone and E.J. Dolan, The Effects of Nuclear Weapons, U.S. Depts. of Defense and Energy, Washington, DC, 3rd Edition, (1977), p. 41.
11. S.B. Martin, "The Role of Fire in Nuclear Warfare," Final Report URS 764 DNA 2692 F, for Contract DASA 01-69-C-0025, NWER Subtask NA 005-01, for Defense Nuclear Agency, Washington, DC 20305. Prepared by U.R.S. Research Company, San Mateo, CA (1974).
12. S.B. Martin, "Experiments on Extinction of Fires by Airblast," Annual Report, Contract DCPA01-79-C-0245, FEMA WU 2564A, SRI International, Menlo Park, CA (1980).
13. J. Backovsky, S. Martin and R. McKee, "Blast Effects on Fires," Annual Report, Contract DCPA01-79-C-0245, FEMA WU 2564A, SRI International, Menlo Park, CA (1980).
14. J. Backovsky, S.B. Martin and R. McKee, "Experimental Extinguishment of Fire by Blast," Final Report, Contract EMW-C-0559, FEMA WU 2564A, SRI International, Menlo Park, CA (1982).

15. F.A. Williams, "Mechanisms of Fire Spread," pp. 1281-1294, Sixteenth Symposium (International) on Combustion, The Combustion Institute, Pittsburgh, PA (1976).
16. T.J. Ohlemiller and F.E. Rogers, "Cellulose Insulation Material. Effect of Additives on Some Smolder Characteristics," Combustion Science and Technology, 24, pp. 139-152, (1980).
17. K.N. Palmer, "Smoldering Combustion in Dusts and Fibrous Materials," Combustion and Flame, 1, pp. 129-154, (1957).
18. J.N. deRis, "Spread of a Laminar Diffusion Flame," pp. 241-252, Twelfth Symposium (International) on Combustion, The Combustion Institute, Pittsburgh, PA (1969).
19. A.C.F. Pello, "A Theoretical Model for the Upward Laminar Spread of Flames over Vertical Fuel Surfaces," Combustion and Flame, 31, pp. 135-148, (1978).
20. L. Orloff, J. deRis and G.H. Markstein, "Upward Turbulent Fire Spread and Burning of Fuel Surface," Fifteenth Symposium (International) on Combustion, The Combustion Institute, Pittsburgh, PA (1976).
21. M. Sibuhn and J. Kim, "The Dependence of Flame Propagation on Surface Heat Transfer: II Upward Burning," Unpublished Note (Circa 1976).
22. M. Vogel and F.A. Williams, "Flame Propagation along Matchstick Arrays," Combustion Science and Technology, 1, pp. 429-436, (1970).
23. H.W. Emmons and T. Shen, "Fire Spread in Paper Arrays," pp. 917-926, Thirteenth Symp. (International) on Combustion, The Combustion Institute, Pittsburgh, PA (1971).
24. S. Atallah, "Model Studies on the Propagation of Fire," Chem. E. Thesis, MIT (1960). Also see S. Atallah, "Model Studies of a Forest Fire," WSS/CI Paper No. 64-9, 1964 Spring Meeting, Western States Section, The Combustion Institute, Stanford University, Stanford, CA (April, 1964).
25. P.H. Thomas, "Buoyant Diffusion Flames," pp. 381-382, Combustion and Flame, 4, (1960).
26. P.H. Thomas, C.T. Webster and M.M. Raftery, "Some Experiments on Buoyant Diffusion Flames," pp. 359-367, Combustion and Flame, 5, (1961).
27. P.H. Thomas, "The Size of Flames from Natural Fires," pp. 844-859, Ninth Symposium (International) on Combustion, The Combustion Institute, Pittsburgh, PA (1963).
28. F.R. Steward, "Linear Flame Heights for Various Fuels," pp. 171-178, Combustion and Flame, 8, (1964).

29. F.R. Steward, "Prediction of the Height of Turbulent Diffusion Buoyant Flames," pp. 203-212, Combustion Science and Technology, 2, (1970).
30. H.W. Emmons, "Fire in the Forest," Fire Research Abstracts and Reviews, 5(3), pp. 163-178, (1963).
31. J.R. Welker, O.A. Pipkin and C.M. Sliepcevich, "The Effect of Wind on Flames," Fire Technology, 1(2), pp. 122-129, (1965).
32. M. Hamada, "Study of Inclination of Flame Due to Wind," Bulletin of Fire Protection Society of Japan, 1(2), pp. 41-43, (1952).
33. J.R. Welker and C.M. Sliepcevich, "Burning Rates and Heat Transfer from Wind-Blown Flames," Fire Technology, 2(3), pp. 211-218, (1966).
34. K.S. Mudan and P.A. Croce, "A Thermal Radiation Model for LNG Trench Fires," Paper Presented at the 1984 Winter Annual Meeting of ASME, New Orleans, LA (December, 1984).
35. R.C. Rothermel, "A Mathematical Model for Predicting Fire Spread in Wildland Fuels," USDA Forest Service Research Paper INT-115, Intermountain Forest and Range Experiment Station, Ogden, UT (January, 1972).
36. M. Law, "Heat Radiation from Fires and Building Separation," Fire Research Technical Paper No. 5, Dept. of Scientific and Industrial Research and Fire Offices' Committee, Joint Fire Research Organization, HMSO, London, (1963).
37. R. Siegel and J.R. Howell, Thermal Radiation Heat Transfer, McGraw-Hill Book Co., New York, NY (1981).
38. R.S. Alger, Unpublished work, U.S. Naval Radiological Defense Laboratory, San Francisco, CA (1966).
39. W.J. Parker, "Urban Mass Fire Scaling Considerations," Report, OCD Work Unit No. 2536F, USNRDL-TR-67-150, U.S. Naval Radiological Defense Laboratory, San Francisco, CA (1967).
40. C.H.B. Priestley and F.K. Ball, "Continuous Convection from an Isolated Source of Heat," pp. 144-157, Quarterly Journal of the Royal Meteorological Society, 81, (1955).
41. B.R. Morton, Sir G. Taylor and J.S. Turner, "Turbulent Gravitational Convection from Maintained and Instantaneous Sources," pp. 1-23, Proceedings of the Royal Society, Series A, 234(1196), (1956).
42. H. Rouse, C.S. Yih and H.W. Humphreys, "Gravitational Convection from a Boundary Source," Tellus, 4, pp. 201-210, (1952).
43. R.L. Alpert, "Fire-Induced Turbulent Jet," FMRC Report Serial No. 19722-2, Factory Mutual Research Corporation, Norwood, MA (1971).



44. G.I. Taylor, "Fire Under Influence of Natural Convection," pp. 10-31, in The Use of Models in Fire Research, W.G. Berl, Editor, Publication No. 786, National Academy of Sciences--National Research Council, Washington, DC (1961).
45. S.L. Lee and H.W. Emmons, "A Study of Natural Convection above a Line Fire," pp. 353-369, Journal of Fluid Mechanics, 11, (1961).
46. H.C. Hottel, "Fire Modeling," pp. 32-47, in The Use of Models in Fire Research, W.G. Berl, Editor, Publication No. 786, National Academy of Sciences -- National Research Council, Washington, D.C. (1961).  
  
Also see: H.C. Hottel, "Modeling Principles in Relation to Fire," pp. 2-4, Fire Research Abstracts and Reviews, 2(1), (1960).
47. M.P. Murgai, "Radiative Transfer Effects in Natural Convection Above Fires," pp. 441-448, Journal of Fluid Mechanics, 12, (1962).  
  
Also see: pp. 180-182, Fire Research Abstracts and Reviews, 4(3), (1962).
48. B.R. Morton, "Modeling Fire Plumes," pp. 973-982, Tenth Symposium (International) on Combustion, The Combustion Institute, Pittsburgh, PA (1965).
49. H.J. Nielsen and L.N. Tao, "The Fire Plume Above a Large Free-Burning Fire," pp. 965-972, Tenth Symposium (International) on Combustion, The Combustion Institute, Pittsburgh, PA (1965).
50. J. Faure, "Study of Convection Currents Created by Fires of Large Area," pp. 130-149, in The Use of Models in Fire Research, W.G. Berl, Editor, Publication No. 786, National Academy of Sciences -- National Research Council, Washington, D.C. (1961).
51. G.M. Byram, "Scaling Laws for Modeling Mass Fires," Western States Section/The Combustion Institute, Paper No. WSCI 66-15, (1966).
52. S.L. Lee and C.H. Ling, "Natural Convection Plume Above a Circular Ring Fire," pp. 501-506, Eleventh Symposium (International) on Combustion, The Combustion Institute, Pittsburgh, PA (1967).
53. W.J. Parker, R.C. Corlett and B.T. Lee, "An Experimental Test of Mass Fire Scaling Principles," Paper No. WSCI 68-14, Western States Section/The Combustion Institute, University of Southern California, (April, 1968).
54. C.M. Countryman, "Project FLAMBEAU--An Investigation of Mass Fire, 1964-1967," Final Report, Vol. I, OCD WU 2536A, DASA EO-850-68, Pacific Southwest Forest and Range Experiment Station USDA U.S. Forest Service, (1969).
55. C.S. Tarifa, P.P. del Notario and F.G. Moreno, "On the Flight Paths and Lifetimes of Burning Particles of Wood," pp. 1021-1037, Tenth Symposium (International) on Combustion, The Combustion Institute, Pittsburgh, PA (1965).

56. C.S. Tarifa, P.P. del Notario, F.G. Moreno and A.R. Villa, "Transport and Combustion of Firebrands," Final Report of Grants FG-SP-114 and FG-SP-146, to USDA Forest Service, Prepared by Instituto Nacional de Tecnica Aeroespacial, Madrid, Spain, (May, 1967).
57. S.L. Lee and G.M. Hellman, "Firebrand Trajectory Study Using an Empirical Velocity-Dependent Burning Law," pp. 265-274, Combustion and Flame, 15, (1970).
58. A. Muraszew, J.B. Fedele and W.C. Kuby, "Firebrand Investigation," Report No. ATR-75(7470)-1, INT Grant No. 12, USDA Forest Service, Prepared by The Aerospace Research Corporation, El Segundo, CA (1975).
59. B.R. Morton, "Fire and Wind," pp. 75-82, Fire Research Abstracts and Reviews, 8(2), (1966).
60. R.R. Long, "Fire Storms," pp. 53-68, Fire Research Abstracts and Reviews, 9(2), (1967).
61. R.D. Small and H.L. Brode, "Physics of Large Urban Fires," P.S.R. Report 1010, Final Report, Contract No. DCPA01-79-C-0291, WU 2564E, Prepared by Pacific-Sierra Research Corporation, Santa Monica, CA (1980).
62. G.F. Carrier, F.E. Fendell, and P.S. Feldman, "Firestorms," DNA-TR-81-102, Technical Report, Contract No. DNA-001-81-C-0111, Prepared by TRW, Redondo Beach, CA (1982).
53. A. Strasser and J. Grumer, "Air Flows into Uncontrolled Fires," Final Report No. 3909, for Department of Defense and National Science Foundation through the National Bureau of Standards, Prepared by USD Interior, Bureau of Mines, Explosives Research Center, Pittsburgh, PA (1964).
64. M. Leva, M. Weintraub, M. Grumer, M. Pollchik and H.A. Storch, "Fluid Flow Through Packed and Fluidized Systems," Bureau of Mines Bulletin No. 504, Pittsburgh, PA (1951).
65. R.C. Corlett, "Velocity Distributions in Fires," Chapter 5 in Heat Transfer in Fires, P.L. Blackshear, Jr., Editor, Scripta Book Company, Washington, D.C. (1974).
66. P.L. Blackshear, Jr., "Some Thoughts on Heat and Mass Transfer in Very Large Fires," Appendix D, pp. 145-158, in W.J. Parker, "Urban Mass Fire Scaling Considerations," USNRDL-TR-67-150, OCD WU No. 2536F, U.S. Naval Radiological Defense Laboratory, San Francisco, CA (1967).
67. B.D. Wood, P.L. Blackshear, Jr., and E.R.G. Eckert, "Mass Fire Model: An Experimental Study of the Heat Transfer to Liquid Fuel Burning from a Sand-Filled Pan Burner," pp. 113-129, Combustion Science and Technology, 4, (1971).
68. A.A. Putnam and C.F. Speich, "A Model Study of the Interaction of Multiple Turbulent Diffusion Flames," pp. 867-877, Ninth Symposium (International) on Combustion, The Combustion Institute, Pittsburgh, PA (1963).

69. A.M. Kanury, "Rate of Charring Combustion in a Fire," pp. 1131-1142, Fourteenth Symposium (International) on Combustion, The Combustion Institute, Pittsburgh, PA (1973).

## APPENDIX

### GLOSSARY OF TERMS

The multitude of fire studies, from which scaling relationships are drawn here, frustrate all deliberate attempts to unify the nomenclature. A section-by-section nomenclature appears to be desirable to avoid ambiguities notwithstanding some certain redundancy.

#### Section 5:

- c a constant coefficient, Table I.
- D distance from ground-zero, m.
- $E_{\text{total}}$  thermal radiation yield, J.
- f thermal radiant energy partition  $\equiv E_{\text{total}}/W$ .
- F a function.
- $\hat{F}$  fluence,  $\text{J/m}^2$ .
- H height of burst, m.
- I irradiance at the target,  $\text{W/m}^2$ .
- m an index, Table I.
- n an index, Table I.
- P thermal energy release rate, W.
- R radius, m.
- t time, s.
- T temperature of the fireball, K.
- W weapon yield, J.
- $\kappa$  absorption coefficient of air,  $1/\text{m}$ .
- $\rho$  density of air,  $\text{kg/m}^3$ .
- $\rho_0$  density of air at sea level,  $\text{kg/m}^3$ .
- $\sigma$  Stefan-Boltzmann Constant,  $\text{W/m}^2\text{K}^4$ .
- $\tau$  transmissivity of air mass.

Section 6:

$C_{ps}$	specific heat of the solid, J/kg K.
$g$	gravitational acceleration, m/s <sup>2</sup> .
$h$	convective heat transfer coefficient, W/m <sup>2</sup> K.
$H$	height of the target specimen, m.
$I$	irradiance on target surface, W/m <sup>2</sup> .
$K_s$	thermal conductivity of the solid, W/mK.
$l$	solid target specimen thickness, m.
$t$	time, s.
$T_0$	initial temperature, K.
$T_p$	pyrolysis temperature, K.
$T_\infty$	ambient gas temperature, K.
$T^*$	ignition temperature, K.
$\alpha_s$	solid thermal diffusivity, m <sup>2</sup> /s.
$\epsilon'_s$	solid surface emissivity.
$\nu_g$	gas-phase kinematic viscosity, m <sup>2</sup> /s.
$\rho_s$	solid density, kg/m <sup>3</sup> .

Section 7:

$C_{pg}$	gas-phase specific heat, J/kg K.
$E$	activation energy of oxidation reaction, J/kgmole.
$h_c$	enthalpy of combustion, J/kg.
$k_0$	preexponential factor of oxidation reaction, 1/s.
$l$	fuel bed length along the flow direction, m.
$P$	Damkohler number.
$q$	energetic potency parameter.
$R$	universal gas constant, J/kgmole K.

$u$  blast wind peak velocity, m/s.  
 $Y_{F1}$  fuel vapor mass fraction at the fuel surface.

Section 8

Subsection 8.1:

$B_i$  Biot number.  
 $C_{ps}$  solid specific heat, J/kg K.  
 $D$  diffusivity of gases through porous solid,  $m^2/s$ .  
 $\hat{D}$  nondimensional diffusivity  $D$ .  
 $E$  activation energy of smolder reaction, J/kgmole.  
 $f$  stoichiometric fuel/oxygen mass ratio, kg/kg.  
 $h$  convective heat loss coefficient,  $W/m^2K$ .  
 $h_c$  enthalpy of smoldering combustion, J/kgmole.  
 $K, K_s$  solid thermal conductivity, W/mK.  
 $\lambda, \lambda_s$  solid half-thickness, m.  
 $R$  universal gas constant, J/kgmoleK.  
 $t$  time, s.  
 $T_p$  pyrolysis temperature, K.  
 $u$  smolder spread velocity, m/s.  
 $V$  nondimensional  $u$ .  
 $Y_{O\infty}$  oxygen mass fraction in ambient gas.  
 $Z$  characteristic smolder reaction rate, kgmole/ $m^3s$ .  
 $\delta$  a Damkohler number.  
 $\rho_c$  char density,  $kg/m^3$ .  
 $\rho_g$  gas density,  $kg/m^3$ .  
 $\rho_s$  virgin solid density,  $kg/m^3$ .  
 $\theta_\infty$  nondimensional ambient temperature.

Subsection 8.2:

$C_{pg}$	gas phase specific heat, J/kg K.
$C_{ps}$	solid specific heat, J/kg K.
$h$	gas phase convective heat transfer coefficient, W/m <sup>2</sup> K.
$\Delta h_s$	solid enthalpy rise from initial to ignition state, J/kg.
$K_g$	gas thermal conductivity, W/mK.
$K_{sy}$	solid conductivity in normal direction, W/mK.
$l_g$	gas phase conduction length, m.
$l_s$	thin fuel bed thickness, m.
$l_1$	characteristic length of relevance to $R_1$ , m.
$\dot{q}''$	heat flux across the surface of flame inception, W/m <sup>2</sup> .
$\dot{q}''_g$	gas phase conduction flux, W/m <sup>2</sup> .
$R_1, R_2$	upstream and downstream radiant fluxes, W/m <sup>2</sup> .
$t$	time, s.
$T_f$	flame temperature, K.
$T_{vap}$	vaporization or pyrolysis temperature, K.
$T_\infty$	ambient gas temperature, K.
$u$	flame spread velocity, m/s.
$u_g$	opposing ambient wind speed, m/s.
$z$	a dummy parameter of relevance to $R_1$ .
$\alpha_s$	solid thermal diffusivity, m <sup>2</sup> /s.
$\rho_g$	ambient gas density, kg/m <sup>3</sup> .
$\rho_s$	fuel bed solid density, kg/m <sup>3</sup> .

Subsection 8.3:

$B$	transfer number.
-----	------------------

$C_{pg}$	gas specific heat, J/kg K.
$C_{ps}$	solid specific heat, J/kg K.
$f$	stoichiometric fuel/oxygen mass ratio, kg/kg.
$g$	gravitational force per unit mass, m/s <sup>2</sup> .
$G$	Galileo number.
$h_c$	heat of combustion, J/kg.
$j$	an index of 1 for laminar flow and of 0 for turbulent flow.
$K_{g\infty}$	ambient gas conductivity, W/mK.
$z$	distance along the bed from the origin fixed at the original ignition front, m.
$L$	latent heat of pyrolysis, J/kg.
$\dot{m}'_f$	pyrolyzate transpiration rate per unit fuel bed width, kg/ms.
$\dot{m}''$	pyrolyzate mass flux, kg/m <sup>2</sup> s.
$n$	an index.
$\dot{q}'_F$	upstream heat flow rate per unit fuel bed width, W/m.
$\dot{q}'_c$	combustive heat release rate per unit fuel bed width, W/m.
$\dot{q}''$	heat flux, W/m <sup>2</sup> .
$T_{g\infty}, T_\infty$	ambient gas temperature, K.
$T_p$	pyrolysis temperature, K.
$T_s$	solid surface temperature, K.
$u$	flame spread velocity, m/s.
$V$	nondimensional flame spread velocity.
$x_b$	length of fuel bed between pyrolysis and burnout fronts, m.
$x_p$	location of pyrolysis front, m.
$Y_{O\infty}$	ambient gas oxygen mass fraction.
$\nu_{g\infty}$	ambient gas kinematic viscosity, m <sup>2</sup> /s.



- $\phi$  a nondimensional ratio of heat to mass fluxes in Sibuklin analysis.
- $\rho_s$  solid density,  $\text{kg/m}^3$ .

Subsection 8.4:

- A, B, C, D Atallah's forest fire spread nondimensional parameters.
- $\bar{A}, \bar{B}, \bar{C}, \bar{D}$  modified Atallah parameters.
- $C_p, C_{ps}$  solid fuel specific heat,  $\text{J/kg K}$ .
- $d, d_0$  fire base diameter, m.
- E plume dynamics nondimensional parameter.
- f Welker's flame shape factor.
- F fuel bed structure parameter.
- Fr Froude number.
- g gravitational constant,  $\text{m/s}^2$ .
- g Emmon's firebreak width, m.
- $\bar{h}$  convective heat loss coefficient,  $\text{W/m}^2\text{K}$ .
- $h_c$  heat of combustion,  $\text{J/kg}$ .
- H Atallah's flame height, m.
- H Emmons/Shen paper strip height, m.
- k entrainment/mixing constant.
- K a constant in Welker's work.
- $K_g$  gas conductivity,  $\text{W/mK}$ .
- $K, K_s$  solid conductivity,  $\text{W/mK}$ .
- $z$  stick height, m.
- $z_g$  gas phase conduction length, m.
- $L_f$  Emmons/Shen flame height, m.

$m''$	fuel loading per unit area, $\text{kg/m}^2$ .
$\dot{m}''$	average burning rate, $\text{kg/m}^2\text{s}$ .
$\dot{m}_0$	gaseous fuel feed rate, $\text{kg/s}$ .
$m$	an index.
$M_f$	fuel moisture content, $\text{kg/kg}$ .
$n$	an index in Vogel/Williams work, $1/4$ for laminar flames and $0$ for turbulent flames.
$n$	an index.
$P$	Emmon's burning intensity parameter.
$Q_b$	radiant emission intensity per unit width, $\text{W/m}$ .
$Q_i$	ignition energy, $\text{J/kg}$ .
$Q'$	heat output rate per unit length of a line fire, $\text{W/m}$ .
$\dot{Q}$	heat release rate, $\text{W}$ .
$r$	Vogel/Williams downward flame propagation speed on a stick, $\text{m/s}$ .
$r$	Steward's stoichiometric air/fuel mass ratio, $\text{kg/kg}$ .
$R$	Emmon's nondimensional fire spread velocity.
$s$	stick spacing, $\text{m}$ .
$S$	spacing of paper strips, $\text{m}$ .
$t_i$	time to ignition, $\text{s}$ .
$T_i$	ignition temperature, $\text{K}$ .
$T_f$	flame temperature, $\text{K}$ .
$T_g$	gas temperature, $\text{K}$ .
$T_0$	solid initial temperature, $\text{K}$ .
$T_p$	pyrolysis temperature, $\text{K}$ .
$T_\infty$	ambient gas temperature, $\text{K}$ .
$\Delta T$	$T_f - T_\infty$ , $\text{K}$ .

$u$  flame spread velocity, m/s.  
 $u_g$  fuel feed velocity, m/s.  
 $u_{tip}$  flame gas velocity at the flame tip, m/s.  
 $V$  nondimensional flame spread velocity.  
 $v$  wind speed, m/s.  
 $\dot{V}$  volumetric fuel feed rate, m<sup>3</sup>/s.  
 $w$  line fire width, m.  
 $w$  width of burning zone, m.  
 $w_i$  ignition strip width, m.  
 $x$  distance down stream, m.  
 $x_f$  flame tip height, m.  
 $y^*$  flame stand-off distance, m.  
 $z$  height from floor, m.  
 $\alpha$  Emmons' fuel bed surface/volume ratio, 1/m.  
 $\alpha_s$  solid thermal diffusivity, m<sup>2</sup>/s.  
 $\beta$  Rothermel's porous bed packing ratio.  
 $\beta_v$  volumetric expansion coefficient, 1/K.  
 $\epsilon$  an effective heating number.  
 $\epsilon_f$  flame emissivity.  
 $\epsilon_s$  solid surface emissivity.  
 $\theta$  angle of tilt of a wind-blown flame.  
 $\nu_a$  ambient gas dynamic viscosity, kg/ms.  
 $\xi$  Rothermel's propagation flux ratio.  
 $\rho, \rho_s$  solid density, kg/m<sup>3</sup>.  
 $\rho_b$  Rothermel's solid bulk density, kg/m<sup>3</sup>.  
 $\rho_0$  inlet fuel density, kg/m<sup>3</sup>.

$\rho_a, \rho_\infty$  ambient air density,  $\text{kg/m}^3$ .  
 $\rho_f$  flame gas density,  $\text{kg/m}^3$ .  
 $\sigma$  Rothermel's fuel particle surface/volume ratio,  $1/\text{m}$ .  
 $\sigma$  Stefan-Boltzmann Constant,  $\text{W/m}^2\text{K}^4$ .  
 $\tau$  Emmons/Shen paper thickness,  $\text{m}$ .  
 $\tau$  forest fuel bed height,  $\text{m}$ .  
 $\tau$  fuel bed thickness, height of a tree,  $\text{m}$ .  
 $\phi$  nondimensional density defect parameter.  
 $\phi_s$  slope factor.  
 $\phi_w$  wind factor.

Subsection 8.5:

$\bar{A}$  ceiling + soffitt skirt area,  $\text{m}^2$ .  
 $C_{pg}$  gas specific heat,  $\text{J/kg K}$ .  
 $C_{pw}$  wall-lining specific heat,  $\text{J/kg K}$ .  
 $f$  area covered by a flame of a given power,  $\text{m}^2/\text{kW}$ .  
 $h$  convective heat transfer coefficient between the flame  
 and wall,  $\text{W/m}^2\text{K}$ .  
 $\bar{h}$  convective + radiative heat transfer coefficient between  
 the hot gases and wall-lining,  $\text{W/m}^2\text{K}$ .  
 $H_0$  window height,  $\text{m}$ .  
 $I$  radiant flux imposed in a heat release rate calorimeter,  $\text{W/m}^2$ .  
 $k$  a window flow constant,  $\approx 1.6 \text{ kg/m}^{5/2}\text{s}$ .  
 $K_w$  wall-lining conductivity,  $\text{W/mK}$ .  
 $\dot{m}_a$  air flow rate,  $\text{kg/s}$ .  
 $\dot{m}_g$  product gas outflow rate,  $\text{kg/s}$ .

$\dot{m}_v$  fuel feed rate, kg/s.  
 $q$  measured heat release rate, W/m<sup>2</sup>.  
 $t$  time, s.  
 $T_a, T_\infty$  ambient air and initial temperature, K.  
 $T_g$  gas temperature, K.  
 $T_w$  wall surface temperature, K.  
 $W_0$  window width, m.  
 $\beta$  wall-lining combustibility parameter.  
 $\gamma$  ceiling + Soffitt skirt area parameter.  
 $\theta_g$  nondimensional gas temperature.  
 $\theta_w$  nondimensional wall surface temperature.  
 $\rho_w$  wall-lining density, kg/m<sup>3</sup>.  
 $\tau$  nondimensional time.  
 $\phi$  nondimensional fuel feed rate.  
 $\phi$  nondimensional air flow rate.  
 $\psi$  window aspect ratio.  
 $\Omega$  wall-lining heating characteristic.

Subsection 8.6:

$I_c$  critical irradiance for ignition, W/m<sup>2</sup>.  
 $I_0$  emission intensity of a fire, W/m<sup>2</sup>.  
 $F_{n-f}$  radiation view factor from nth window flame to target facade f.  
 $n$  window number.  
 $N$  total windows.

Section 9  
Subsection 9.1:

A	source energy strength, $\text{m}^3\text{K/s}$ .
b	a measure of plume thickness, m.
c	plume spreading constant $\equiv dR/dz$ .
g	gravitational acceleration, $\text{m/s}^2$ .
Q	buoyancy source, $\text{m}^4/\text{s}^3$ .
r	radial location, m.
R	radius of plume at any height z, m.
$R_0$	plume source radius, m.
T	temperature at any (z,r), K.
$T_0$	source temperature, K.
$T_\infty$	ambient temperature, K.
$T_{\max}$	maximum temperature at any z, K.
w	axial velocity at any (z,r), m/s.
$w_0$	source axial velocity, m/s.
$w_{\max}$	maximum axial velocity at any z, m/s.
W	nondimensional axial velocity.
z	axial location, m.
$z_0$	distance of virtual point source below the finite real source, m.
$z_{\text{ceiling}}$	ceiling height in stable atmosphere, m.
$\alpha$	entrainment constant.
$\beta$	Rouse constant = 96/71.
$\gamma$	stratification number.
$\theta$	nondimensional temperature.

- $\rho$  plume gas density, kg/m<sup>3</sup>.  
 $\rho_{\infty}$  ambient gas density, kg/m<sup>3</sup>.

Subsection 9.2:

- A Morton's nondimensional radiation free path.  
 C Morton's modified Froude number.  
 $C_p$  plume fluid specific heat, J/kg K.  
 D Morton's ratio of radiative loss to convective transport.  
 I a shape factor.  
 $P_{\infty}^*$  nondimensional ambient pressure.  
 $\dot{q}$  power of the buoyancy source, W.  
 u radial velocity, m/s.  
 $u_e$  entrainment velocity, m/s.  
 $\alpha_w$  weakly buoyant plume entrainment constant.  
 $\alpha^*$  a constant.  
 $\gamma$  adiabatic exponent.  
 $\kappa$  plume gas absorption coefficient, 1/m.  
 $\sigma$  Stefan-Boltzmann Constant, W/m<sup>2</sup>K<sup>4</sup>.  
 $\phi$  Murgai's radiation number.

Subsection 9.3:

- L fire-base scale, m.  
 $r_0$  mean radius of the ring-fire-base, m.  
 U nondimensional radial velocity.  
 W nondimensional axial velocity.  
 $w$  characteristic velocity, m/s.

Subsection 9.4:

A	frontal area of the flying brand, $m^2$ .
$C_D$	drag coefficient.
g	gravitational constant, $m/s^2$ .
m	mass of the firebrand, kg.
r	radius of the firebrand, m.
$r_0$	initial radius of the firebrand, m.
Re	Reynolds number of flight.
t	time, s.
$t_b$	burnout time, s.
$t_g$	time of flight, s.
$U_1$	a nondimensional parameter.
$w_f$	fall velocity, m/s.
$w_{f0}$	initial fall velocity, m/s.
$\beta, \delta$	empirical combustion constants, $1/s^2$ and m.
$\zeta$	density ratio $\rho_\infty/\rho_{w0}$ .
$\eta$	an empirical combustion constant, $1/s^2$ .
$\lambda_1, \lambda_2$	length ratios.
$\rho_\infty$	ambient air density, $kg/m^3$ .
$\rho_w$	wood density, $kg/m^3$ .
$\rho_{w0}$	initial wood density, $kg/m^3$ .
x	nondimensional time.

Subsection 9.5:

$C_p$	isobaric heat capacity, J/kg K.
$C_v$	isochoric heat capacity, J/kg K.



$d$	fire diameter, m.
$F$	nondimensional circulation parameter.
$g$	gravity, $m/s^2$ .
$k$	building or tree height, m.
$k'$	surface roughness ratio $k/d$ .
$L$	a characteristic length, m.
$m$	a thermodynamic parameter.
$P$	pressure, Pa.
$\bar{P}_0$	potential pressure of the atmosphere, Pa.
$r$	radius, m.
$s$	$\Delta\bar{\rho}/\bar{\rho}_0$
$t$	time, s.
$v$	velocity, m/s.
$\alpha$	a constant.
$\epsilon$	nondimensional gradient of potential density with height.
$\rho$	density, $kg/m^3$ .
$\bar{\rho}$	potential density, $kg/m^3$ .
$\bar{\rho}_0$	potential density of ambient air, $kg/m^3$ .
$\Delta\bar{\rho}$	$\bar{\rho}_0 - \bar{\rho}$ , $kg/m^3$ .
$\sigma$	adiabatic exponent, $C_p/C_v$ .
$\Omega$	ambient air angular velocity, $1/s$ .

Subsection 9.6:

$C_{p\infty}$  ambient air specific heat, J/kg K.

$C_{pg}$  gas specific heat, J/kg K.

$d, d_{particle}, \lambda$  particle diameter, m.

$d_0$  particle initial diameter, m.  
 $d_{bed}, \ell$  bed diameter, m.  
 $f$  friction factor.  
 $g$  gravity,  $m/s^2$ .  
 $h$  convective heat transfer coefficient,  $W/m^2K$ .  
 $H_{bed}$  bed height, m.  
 $j$  an index, 0, 1, 2 respectively for slab, cylinder and sphere.  
 $K_g$  gas conductivity,  $W/mK$ .  
 $\ell$  bed dimension, m; also particle size, m.  
 $\ell_0$   $d_0/2$ , half-thickness of the particle, m.  
 $L_{sg}$  solid-to-gas phase change latent heat,  $J/kg$ .  
 $m$  mass of particle, kg.  
 $m_0$  initial mass, kg.  
 $\dot{m}_F$  burning rate,  $kg/s$ .  
 $\dot{m}_{max}$  maximum burning rate,  $kg/s$ .  
 $\dot{m}''$  mass flux,  $kg/m^2s$ .  
 $\dot{q}''$  heat feed-back flux,  $W/m^2$ .  
 $\dot{q}''_{rad}$  radiant heat flux,  $W/m^2$ .  
 $\tilde{Q}$  nondimensional heat flux.  
 $t$  time, s.  
 $t^*$  characteristic pyrolysis time, s.  
 $T_b$  burned gas temperature, K.  
 $T_\infty$  hot gas, flame, or ambient temperature, K.  
 $T_p'$  pyrolysis temperature, K.  
 $T_0$  fuel initial temperature, K.

$T_w$        evaporating fuel surface temperature, K.  
 $U_{induced}$    induced wind velocity, m/s.  
 $\alpha_0$        virgin solid fuel thermal diffusivity,  $m^2/s$ .  
 $\delta$        fuel bed void fraction.  
 $\lambda$        particle shape factor.  
 $\rho_0$        initial wood density,  $kg/m^3$ .  
 $\rho_c$        final char density,  $kg/m^3$ .  
 $\rho_{\infty}$        ambient air density,  $kg/m^3$ .

## DISTRIBUTION LIST

### DEPARTMENT OF DEFENSE

DEFENSE INTELLIGENCE AGENCY  
ATTN: DB-4C2 C WIEHLE  
ATTN: RTS-2B  
ATTN: WDB-4CR

DEFENSE NUCLEAR AGENCY  
2 CYS ATTN: SPTD  
ATTN: STSP  
4 CYS ATTN: STTI-CA

DEFENSE TECHNICAL INFORMATION CENTER  
12 CYS ATTN: DD

FIELD COMMAND DEFENSE NUCLEAR AGENCY  
ATTN: FCTT W SUMMA  
ATTN: FCTXE

JOINT STRAT TGT PLANNING STAFF  
ATTN: JLKS

### DEPARTMENT OF ENERGY

UNIVERSITY OF CALIFORNIA  
LAWRENCE LIVERMORE NATIONAL LAB  
ATTN: B BOWMAN  
ATTN: J BACKORSKY  
ATTN: J PENNER  
ATTN: R HICKMAN  
ATTN: R PERRETT

LOS ALAMOS NATIONAL LABORATORY  
ATTN: DR. D CAGLIOSTRO  
ATTN: J CHAPIAK

### OTHER GOVERNMENT

DEPARTMENT OF COMMERCE  
ATTN: G MULHOLLAND  
ATTN: H BAUM  
ATTN: R LEVINE

DIRECTOR FFASR  
ATTN: C CHANDLER

FEDERAL EMERGENCY MANAGEMENT AGENCY  
ATTN: ASST ASSOC DIR FOR RSCH J KERR  
ATTN: H TOVEY  
ATTN: OFC OF RSCH/NP H TOVEY

OFFICE OF EMERGENCY SERVICES  
ATTN: W TONGUET

### DEPARTMENT OF DEFENSE CONTRACTORS

CALIFORNIA RESEARCH & TECHNOLOGY, INC  
ATTN: M ROSENBLATT

UNIVERSITY OF CALIFORNIA  
ATTN: PROF R B WILLIAMSON

CARPENTER RESEARCH CORP  
ATTN: H J CARPENTER

CHARLES SCAWTHORN  
ATTN: C SCAWTHORN

COLORADO STATE UNIV  
ATTN: PROF M POREH

FACTORY MUTUAL RESEARCH CORP  
ATTN: R FRIEDMAN

HARVARD UNIVERSITY  
ATTN: PROF G CARRIER

IIT RESEARCH INSTITUTE  
ATTN: H NAPADENSKY

INSTITUTE FOR DEFENSE ANALYSES  
ATTN: L SCHMIDT

KAMAN SCIENCES CORP  
ATTN: E CONRAD

KAMAN TEMPO  
ATTN: DASIAI

KAMAN TEMPO  
ATTN: DASIAI

MCDONNELL DOUGLAS CORP  
ATTN: J KIRBY  
ATTN: J PECK

UNIVERSITY OF NOTRE DAME DU LAC  
2 CYS ATTN: A KANURY  
ATTN: T J MASON

PACIFIC-SIERRA RESEARCH CORP  
ATTN: H BRODE, CHAIRMAN SAGE  
ATTN: R SMALL

R & D ASSOCIATES  
ATTN: D HOLLIDAY  
ATTN: F GILMORE  
ATTN: P HAAS  
ATTN: R TURCO

RAND CORP  
ATTN: P DAVIS

RAND CORP  
ATTN: B BENNETT

SCIENCE APPLICATIONS INTL CORP  
ATTN: M DRAKE  
ATTN: M MCKAY

SCIENCE APPLICATIONS INTL CORP  
ATTN: D BACON  
ATTN: J COCKAYNE

**DEPT OF DEFENSE CONTRACTORS (CONTINUED)**

SCIENTIFIC SERVICES, INC  
ATTN: C WILTON

STAN MARTIN ASSOCIATES  
ATTN: S MARTIN

SWETL, INC

ATTN: T PALMER

TRW ELECTRONICS & DEFENSE SECTOR

ATTN: F FENDELL